In Situ Synthesis of Iron Oxide within Polyvinylamine Nanoparticles

BY

Zahra Mohammadi
B.S., University of Tehran
Tehran, Iran

Submitted to the graduate degree program in
Chemical and Petroleum Engineering and the Faculty of the
Graduate School of the University of Kansas in partial fulfillment of the
requirements for the degree of Master's of Science.

Prof. Cory Berkland (Chair)

Committee Members:

Prof. Marylee Southard

Prof. Stevin Gehrke

Date Defended:

The Thesis Committee for Zahra Mohammadi certifies
That this is the approved Version of the following thesis:

In Situ Synthesis of Iron Oxide within Polyvinylamine Nanoparticles

Prof. Cory Berkland (Chair)

Committee Members:

Prof. Marylee Southard

Prof. Stevin Gehrke

Date Approved:

Abstract:

Magnetic nanoparticles that display high saturation magnetization and high magnetic susceptibility with a size less than 200 nm are of great interest for medical applications. Investigations of magnetic nanoparticles have been increasing over the last decade. Magnetite nanoparticles are particularly desirable since the biocompatibility of these particles has already been proven. Several synthetic and natural polymers have been employed to stabilize magnetite nanoparticles and enhance their function in vivo. The goal of this work has been to develop a unique methodology for synthesizing magnetite within polymer nanoparticle dispersions so that the resultant magnetite-polymer particles may be used in a range of biomedical applications, specifically as an MRI contrast agent. A method was developed for preparing ≈150 nm polyvinylamine (PVAm) nanoparticles containing iron oxide. These polymeric nanoparticles offer colloidal stability and reactive primary amines for drug conjugation or surface modification.

The polymer-magnetite nanoparticles described in this thesis exhibited a maximum of 12% wt. magnetite and a saturation magnetization of ~30 emu/mg. Transmission electron microscopy (TEM) images showed that the dispersions contained ≈100 to 150 nm diameter PVAm nanoparticles incorporated with iron oxide particles with a size less than ≈10 nm. The ability to synthesize iron oxide inside functionalized polymeric nanoparticles offers

an effective approach to prevent nanoparticle agglomeration and the potential to enable ligand grafting. Stabilized magnetic PVAm nanoparticles may provide a unique synthetic approach to enhance MRI contrast and may offer a platform for molecular imaging.

This research is dedicated to

my son, Ali and my Husband, M. Hosein.

Each page I have written represents time spent away from them.

Acknowledgment

I would like to express my deepest gratitude and sincere appreciation to my thesis advisor, Prof. Cory Berkland, for his great guidance and enthusiasm he has shown during this study. I would also like to thank the members of my committee, Prof. Marylee Southard and Prof. Stevin Gehrke for their valuable comments and suggestions.

Special thanks to Professor David Allan Fowle and his graduate student, Arne Sturm, for all of their help and expertise with UV. I also thank Professor C. Russell Middaugh for proving DLS. Additionally, I would like to thank Dr. David Moore and Heather Shinogle from the KU Microscopy & Analytical Imaging Lab for all of their assistance and patience with SEM and TEM imaging. Thanks to Prof. Judy Wu, Prof. Jenn-Tai Liang and Jim Pilch for giving me access to the atomic absorption and the superconductive quantum devices.

Finally, I would like to thank my lab mates for making the lab a very nice place to be and always having the time for discussions and to answer my questions. Special thanks to David Shi for letting me use graphic images he made in his presentations. This work would not have been possible without their endless kindness and help.

Table of Contents

Chapter 1
1. Fundamentals of Magnetic Nanoparticle Synthesis and Characterization Methods
    1.1. Magnetism
    1.2. Synthesis of Magnetic Nanoparticles
        1.2.1. Synthesis of Iron Oxide Nanoparticles via Aqueous co-precipitation
        1.2.1. Synthesis of Iron Oxide Nanoparticles via Microemulsion
    1.3. Stabilization of Iron Oxide Nanoparticles
        1.3.1. Surface Modification of Iron Oxide Nanoparticles with Polymeric Stabilizer
        1.3.2. Surface Modification of Iron Oxide Nanoparticles with non-Polymeric Organic Stabilizer
    1.4. Characterization of Magnetic Nanoparticles
        1.4.1. X-Ray Diffraction (XRD)
        1.4.2. Superconducting Quantum Interference Devices (SQUID)
    1.5. Biomedical Application of Magnetic Nanoparticles
        1.5.1. Drug Delivery
        1.5.2. Magnetic Resonance Imaging (MRI)
            1.5.2.1. Gd(III) Based Contrast Agents
            1.5.2.2. Superparamagnetic Iron Oxide Based Contrast Agent
    1.6. Toxicity Consideration of Magnetic Nanoparticles

Chapter 2
2. Materials and Methods
    2.1. Materials
    2.2. Synthesis of non-Degradable Cross-Linker
    2.3. Synthesis of Poly (N-vinyl Formamide) Nanoparticles
    2.4. Synthesis of Polyvinylamine Nanoparticles
    2.5. Fabrication of Magnetic Polyvinylamine Nanoparticles
    2.6. Characterization
        2.6.1. Size, Size Distribution, Charge and Surface Characterization of Polyvinylamine and Magnetic Polyvinylamine Nanoparticles
            2.6.1.1 Transmission Electron Microscopy (TEM)
            2.6.1.2. Dynamic Light Scattering (DLS)
        2.6.2. Characterization of Magnetic Nanoparticles
            2.6.2.1. Iron Content in Magnetic Nanoparticles (UV & AA)
            2.6.2.2. Magnetization of Magnetic Nanoparticles (SQUID)
            2.6.2.3. Coordination of Iron Oxide in Polymeric Network (FTIR)
            2.6.2.4. Cytotoxicity (MTS Assay)
    2.7. Results and Discussion
        2.7.1. Size and Charge Characterization of PVAm and Magnetic PVAm Nanoparticles

2.7.1.1. Dynamic Light Scattering
2.7.1.2. Transmission Electron Microscopy
2.7.2. Characterization of Magnetic PVAm Nanoparticles
2.7.2.1. Qualification of Iron Oxide Fabricated in Polyvinylamine Nanoparticles
2.7.2.2. Magnetization Results
2.7.2.3. Coordination of Iron Oxide in Nanoparticles (FTIR)
2.7.2.4 Cytotoxicity Results
2.8. Conclusion
2.9. Future Work
3. References
4. Appendix

Chapter 1

Fundamentals of Magnetic Nanoparticles

Introduction:

Magnetic nanoparticles have been intensively studied for their applications in biomedical areas such as enzyme and protein immobilization, targeted drug delivery, magnetically controlled transport of anticancer drugs, *in vitro* cell separations and magnetic resonance (MR) contrast enhancement [1-7]. Several investigations have been carried out in the field of superparamagnetic iron oxide nanoparticles since biocompatibility of these particles has already been proven [8]. In MR imaging, superparamagnetic nanoparticles are especially desirable as they may potentially provide higher contrast enhancement than conventional paramagnetic Gd-based contrast agents [9-12].

The direct use of these particles *in vivo,* however, can result in formation of agglomerates in the blood plasma potentially increasing clearance by macrophages and the risk of occusions [13, 14]. Furthermore, aggregation of iron oxide nanoparticles reduces the superparamagnetic properties [15]. Agglomeration results because the surface energy of iron oxide nanoparticles is greatly increased as the ratio of surface area to volume increases [1]. To overcome this difficulty and to use these particles for biomedical purposes, it is essential to engineer the surface of the nanoparticles with substances that make them stable, biodegradable and non-toxic in physiological conditions. In addition, conjugation or inclusion of complex biological molecules, such as peptides, hormones, vitamins or drugs is desired [16-19].

When considering coating materials for biomedical applications, it is usually required that particles should have a hydrophilic surface and a final size less than 200 nm to ensure extended circulation time in the blood and minimized clearance by macrophages. In addition, a particle sizes more than ≈10 nm is necessary to escape the renal clearance. Several methods have been reported for surface modification of superparamagnetic iron oxide nanoparticles. These methods are reviewed briefly. The alternative synthesis approach reported here included: (1) designing polymeric nanoparticles with hydrophilic characterization and amine functional groups as a metal chelating agent; (2) carrying out the oxidation reaction inside the polymeric network; (3) tailoring the iron concentration inside the polymeric nanoparticles to successfully maintain the stochiometry of the reaction; and (4) fabricating stable magnetic PVAm nanoparticles with narrow size distribution.

In chapter one, a review of magnetic nanoparticle synthesis and characterization methods are discussed. This chapter focuses on iron oxide nanoparticles that display superparamagnetism, the benefits of superparamagnetic iron oxide nanoparticles, conventional and current stabilization techniques, and benefits of superparamagnetic nanoparticles as MRI contrast agents. It also includes the fundamentals of magnetism and biomedical application of magnetic nanoparticles. In chapter two, a novel research approach to fabricate stabilized superparamagnetic nanoparticles is reported. Magnetic polyvinylamine nanoparticles with a narrow size distribution were prepared by

carrying out the oxidation reaction to produce magnetite inside PVAm nanoparticles. PVAm is a water soluble polymer with a relatively high density of reactive amino groups [20] inside and at the surface of polymer nanoparticles, which have been utilized as a chelating agent for heavy metals due to the presence of primary amines [21]. This property was leveraged to coordinate iron ions within PVAm nanoparticles. The iron was then oxidized *in situ* to produce magnetic PVAm nanoparticles.

1. Fundamentals of Magnetic Nanoparticles Synthesis and Characterization

1.1. Magnetism

The magnetic properties of ferromagnetic materials are the result of their aligned unpaired electron spins. These materials retain magnetization even after the removal of an external field. The term superparamagnetic refers to single domain particles that reach magnetization equilibrium at experimental temperature in a relatively short time. The atomic magnetic dipoles of paramagnetic materials have a tendency to align with an external magnetic field. These particles have a small, positive magnetic susceptibility (i.e., ability to strengthen the field they are in), and return to their random orientation in the absence of a magnetic field due to Brownian fluctuations. In contrast, superparamagnetic iron oxide nanoparticles are known to have much larger susceptibilities compared with paramagnetic materials because the entire crystal aligns with the applied field due to their single crystal nature. Their moments align in the direction of magnetic filed when

placed in an external field and enhance the magnetic flux and they retain no magnetization after removal of the external field (Fig. 1).

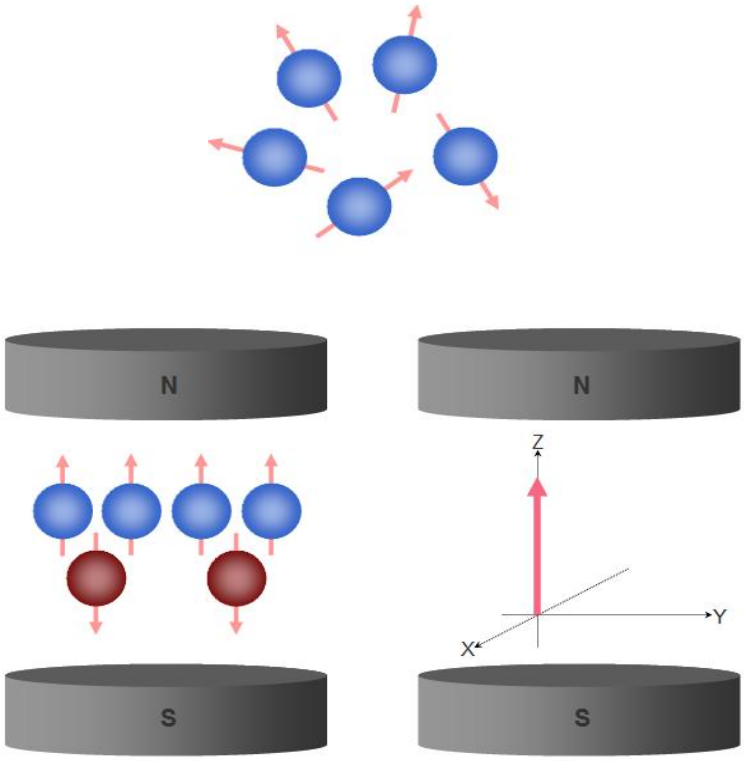

Figure 1. Magnetic moments of magnetic materials in the presence of an applied magnetic field.

1.2. Synthesis of Magnetic Nanoparticles

There are several methods that are generally used to produce magnetic iron oxide nanoparticles. However, the two fundamental approaches currently being used to synthesize magnetite nanoparticles are aqueous co-precipitation and microemulsion.

1.2.1. Synthesis of Iron Oxide Nanoparticles via Aqueous co-precipitation

Conventionally, magnetite is prepared by adding a base to an aqueous mixture of Fe^{2+} and Fe^{3+} chloride at a 1:2 molar ratio. The precipitated magnetite is black in color. Figure 2 shows the chemical reaction of iron ions in the presence of a strong base. The overall reaction is [8, 22]:

$$Fe^{2+} + 2Fe^{3+} + 8OH^{-} \longrightarrow Fe_3O_4 + 4H_2O \qquad (1)$$

A complete precipitation of Fe_3O_4 is expected between pH 9 and 14, while maintaining a 2:1 molar ratio of Fe^{3+}:Fe^{2+} under an oxygen free environment. If the oxygen free environment is not maintained, Fe_3O_4 might be further oxidized as

$$Fe_3O_4 + 0.25\ O_2 + 4.5\ H_2O \longrightarrow 3Fe(OH)_3 \qquad (2)$$

This would critically affect the physical and chemical properties of the magnetic particles. In order to prevent them from possible oxidation in the air as well as from agglomeration, Fe_3O_4 nanoparticles produced by reaction 1 are usually protected by adding organic or inorganic molecules (e.g. surfactants) as a coating agent during the precipitation process. Since the reaction kinetics are strongly related to the oxidation speed of iron species, the synthesis of particles must be done in an oxygen-free environment (e.g. N_2). Bubbling nitrogen gas

through the solution not only protects oxidation of the magnetite but also reduces the particle size when compared to methods that do not remove oxygen [23-25].

Advances in the use of magnetic nanoparticles in biomedical applications depend on the synthetic method, size, size distribution, magnetic properties and the particles' surface characteristics.

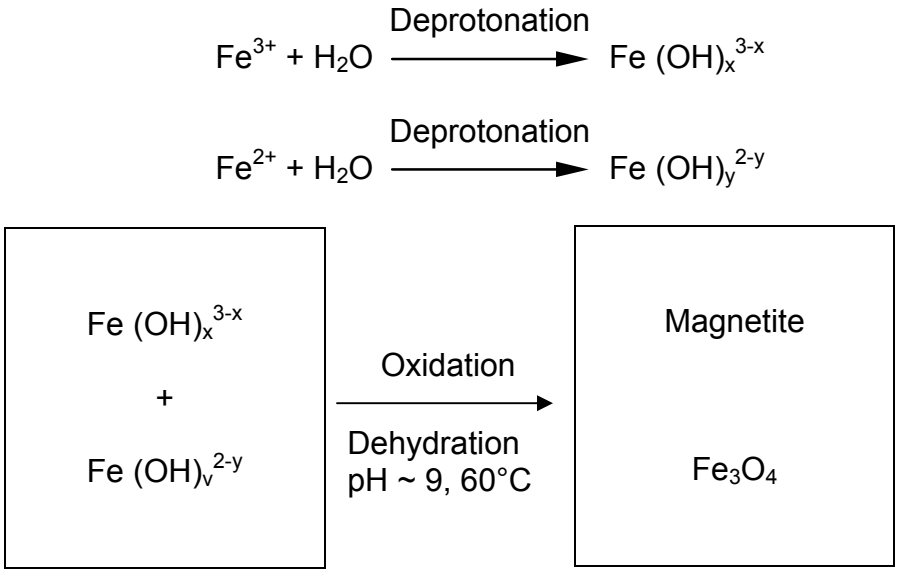

Figure 2. Reaction mechanism of iron oxide formation from an aqueous mixture of ferrous and ferric chloride salts in the presence of a strong base.

Stable aqueous suspensions can be fabricated using various saturated and unsaturated fatty acids as primary and secondary surfactants [26]. In practice, however, little control is actually gained over the size and size distribution of the nanoparticles and, moreover, because of the low concentration of reagent, only small quantities of iron oxide can be obtained.

1.2.2. Synthesis of Iron Oxide Nanoparticles via Microemulsion

A microemulsion is defined as a stable dispersion of two immiscible fluids plus an emulsifier (Fig 3) [27]. This method has recently been used to synthesize superparamagnetic iron oxide nanoparticles. The advantage of this method over previous methods is the control over size and shape of nanoparticles. In oil-in-water microemulsions, nanoparticles are synthesized by suspending a ferrous salt-surfactant precipitate in an aqueous solution. A base is then added to form a magnetic precipitate [28]. In water-in-oil microemulsions, the aqueous phase is dispersed as microdroplets surrounded by a monolayer of surfactant molecules in the continuous inorganic phase [29]. A soluble metal salt is included in the aqueous phase of the microemulsion. A strong base is then added to form the iron oxide precipitate. The superparamagnetic iron oxide nanoparticles are precipitated and oxidized within the nanosized micelle.

The water-in-oil approach is a more common microemulsion synthesis technique for nanoparticles with biomedical applicability. Research shows that this approach results in fairly uniform populations of magnetic nanoparticles [1]. Depending on the solvent in which nanoparticles will be used, an appropriate surfactant can be applied to prevent agglomeration [30]. It should be noted that the homogeneous size of nanoparticles resulting from the microemulsion method is highly dependent on the approach. Poor crystallinity of superparamagnetic nanoparticles fabricated in microemulsions is reported as a disadvantage of this method since it usually reduces the instinct superparamagnetic behavior of nanoparticles [31].

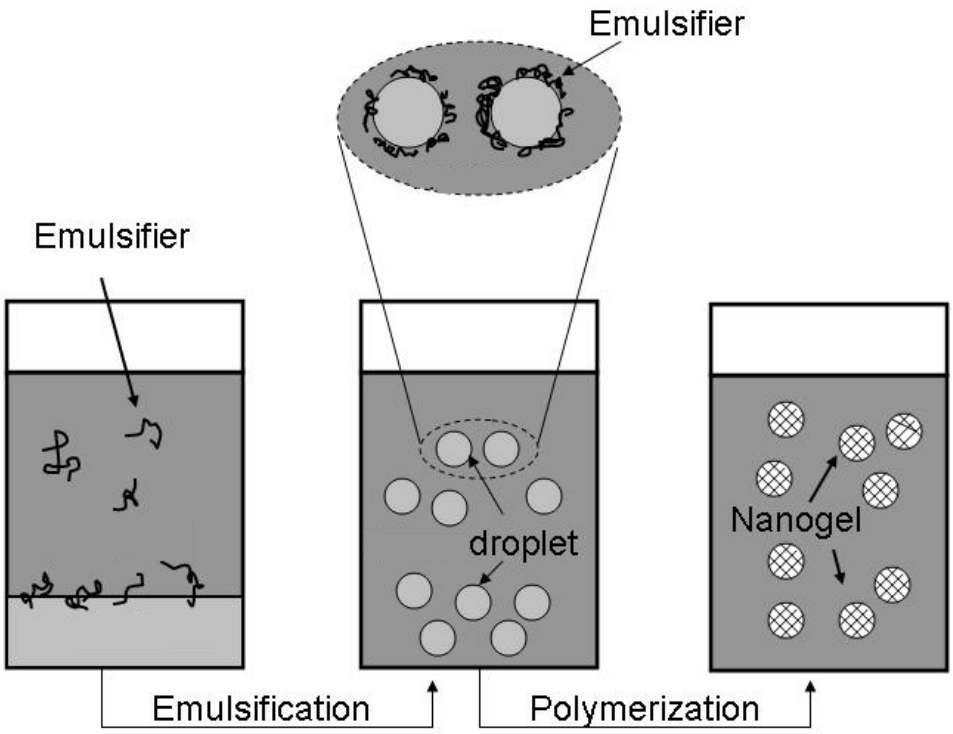

Figure 3. Scheme of a microemulsion reaction in the presence of an emulsifier.

1.3. Stabilization of Iron Oxide Nanoparticles

The stability of the iron oxide nanoparticles in solution is of utmost importance in the preparation and storage process. Magnetic iron oxide particles have hydrophobic surfaces and the ratio of their surface area to volume is relatively high. Due to hydrophobic interactions between the particles, agglomeration can occur resulting in increased particle size. These agglomerates, then, exhibit strong magnetic dipole–dipole attractions between the agglomerated particles and show ferromagnetic behavior [32]. Ferromagnetism is defined as the phenomenon by which materials in an external magnetic field become magnetized and remain magnetized for a period after the material is no longer in

the field. When two large-particle clusters approach one another, both of them come into the magnetic field of the neighbor. Besides the induction of attractive forces between the particles, each particle is in the magnetic field of its neighbor and gets further magnetized [33]. These magnetic particles then adhere, further resulting in a mutual magnetization and propagating agglomeration.

Surface modification of magnetic nanoparticles is often necessary to mitigate magnetic interaction. To prevent the agglomeration of these nanoparticles and enable biomedical applications, it is essential to engineer the surface of the nanoparticles with substances that make them stable in physiological conditions and make them able to conjugate to complex biological molecules [19]. When considering the coating materials, such as polymer or surfactant, for biomedical application, it is usually required that particles should have a hydrophilic, biodegradable and non-toxic surface. To prevent agglomeration of the nanoscale particulate, the coating layer is usually added at the time of preparation. Most of these polymers adhere to surfaces of magnetic nanoparticles. However, to enable these nanoparticles for biomedical applications one should be careful regarding polymer selection as a coating layer. The protecting layer desired for biomedical applications are non-toxic, hydrophilic and biodegradable.

1.3.1. Different Coating Layers to Stabilize Iron Oxide Nanoparticles

Several synthetic and natural polymers have been reported to modify the surface of superparamagnetic nanoparticles to enhance their function *in vivo*. Poly(ethylene-co-vinylacetate), poly(vinylpyrrolidone) (PVP), poly(lactic-co-glycolic acid) (PLGA), poly(ethyleneglycol) (PEG), poly(vinyl alcohol) (PVA), etc. are typical examples of synthetic polymeric systems [1, 34, 35]. Natural polymer systems include use of gelatin, dextran, chitosan, pullulan, etc. Various surfactants, such as sodium oleate and dodecylamine are also usually used to enhance dispersibility of magnetite nanoparticles in an aqueous medium. Use of these materials often resulted in the formation of iron oxide nanoparticles with a wide particle size distribution and poor crystallinity [34]. Table 1 provides a list of materials that have been used as a stabilizer for magnetic nanoparticles with biomedical applications.

Table 1. Different polymer that can be used to stabilize iron oxide nanoparticles.

Polymers/molecules	Advantages	References
Polyethylene glycol (PEG)	Non-covalent immobilization of PEG on the surface improves the biocompatibility, blood circulation time and internalization efficiency of the nanoparticles	[1]
Dextran	Enhances the blood circulation time, stabilizes the colloidal solution	[36]
Polyvinylpyrrolidone (PVP)	Enhances the blood circulation time, stabilizes the colloidal solution	[37]
Polyvinyl alcohol (PVA)	Prevents coagulation of particles, giving rise to monodisperse particles	[38]
Polypeptides	Good for cell biology, e.g. targeting to cells	[39]
Chitosan	A semi-synthesized cationic linear polymer that is widely used as a non-viral gene delivery system; biocompatible, hydrophilic, used in agriculture, food, medicine, biotechnology, textiles, polymers, and water treatment	[40]

1.3.1.1. Surface Modification of Iron Oxide Nanoparticles with Polymer Stabilizers

Stabilization of iron oxide nanoparticles usually takes place during the precipitation of magnetic nanoparticles. This usually prevents agglomeration of nanoparticles and results in monodisperse particle size distributions [36, 40]. A variety of approaches have been reported in the field of iron oxide stabilization. Ugelstad et al. has reported direct precipitation of iron salts inside the pores of microporous polystyrene seeds [41]. The particles obtained had a large size of 2.8-4.5 mm and showed good magnetic properties. In another study, Sauzedde et al. have reported the fabrication of hydrophilic, temperature-sensitive latex magnetic nanoparticles by encapsulating adsorbed iron oxide nanoparticles in an oppositely charged polystyrene-core/poly (N-isopropylacrylamide) shell [42]. In another study, Chatterjee et al. have reported the fabrication of cross-linked albumin magnetic microspheres [43]. Lee et al. have modified the surface of magnetic nanoparticles with PVA by precipitation of iron salts in PVA aqueous solution to form a stable dispersion [44]. They found that the crystallinity of the particles decreased with increasing PVA concentration, while the morphology and particle size remained almost unchanged. Another methodology to stabilize magnetic nanoparticles is through self-assembly of ligand-stabilized nanoparticles into two- and three-dimensionally ordered arrays [45]. Results from this research demonstrated that self-assembly of ligand-stabilized nanoparticles is mainly driven by the interactions of the organic ligands rather than by the interaction of the magnetite cores.

To improve dispersibility, magnetite particles are often modified after precipitation [46]. Gupta et al. have shown that the synthesis of magnetic polymeric nanoparticles with a magnetite core and a polymeric shell is possible using an inverse microemulsion polymerization process [29]. This strategy is based on utilizing the inverse microemulsion approach to modulate the surface of magnetic nanoparticles with PEG. Their results demonstrated that the inverse microemulsion is a better method compared with other bulk precipitation methods to synthesize magnetic polymeric nanoparticles since it offers improved control over iron oxide amount and magnetic properties. Among synthetic polymers, PEG is known to improve the biocompatibility and the blood circulation of magnetic nanoparticles [47]. However, in some cases a poor chemical stability of PEG-modified magnetic nanoparticles has been reported.

1.3.2. Surface Modification with Non-Polymeric Organic Stabilizers (Surfactant)

Because use of polymers can lead to substantial thickness, surface protection using the non-polymeric organic layer, like oleic acid or small monomeric organic molecules, has also been developed as a method to stabilize magnetic nanoparticles [48]. Sahoo et al. have reported the surface protection of magnetite in organic solvent by oleic acid, lauric acid, dodecylphosphonic acid, hexadecylphosphonic acid, and dihexadecylphosphonic acid [49]. They found that alkyl phosphonates and phosphates could be used for obtaining thermodynamically stable dispersions of magnetic nanoparticles. Oleic acid and

stearic acid are similar surfactants which, lead to stability and to precipitation of ferrofluid suspensions respectively. Portet et al. have developed monomeric organic molecules as coating materials to avoid a thick polymeric layer on the surface [30]. These small molecules produce a homogeneous coating on the entire iron oxide core and inhibit protein absorption.

1.4. Characterization of magnetic nanoparticles

Crystal structure and magnetic properties of stabilized magnetic nanoparticles are usually tested to predict their ability to enhance MRI contrast *in vivo*. X-Ray Diffraction (XRD) and superconductive quantum interference devices (SQUID) are usually applied to study the crystallinity and magnetization of particles respectively. These methods are introduced briefly below.

1.4.1. X-Ray Diffraction (XRD)

XRD is a technique used to characterize the crystal structure in polycrystalline or powdered solid samples. Powder diffraction is a type of XRD commonly used to identify unknown substances, by comparing diffraction data against a database maintained by the International Centre for Diffraction Data. These techniques are based on observing the scattered intensity of an x-ray beam hitting a sample as a function of incident and scattered angle, polarization, and wavelength or energy. The peak intensity in XRD result can be used to quantify the proportion of iron oxide forms in a mixture by comparing experimental peak and a reference peak

intensity. The crystal size also can be calculated from line broadening from the XRD pattern using the Scherrer equation.

1.4.2. Superconducting Quantum Interference Devices (SQUID)

The magnetization properties usually are investigated using Superconducting Quantum Interference Device. This device provides fundamental magnetic behavior quantification including saturation magnetization (MS), magnetic remanence (MR), and particle size information. Several other characterization methods are also available to investigate the properties of magnetic particle systems. These methods include vibrating sample magnetometer (VSM) which provides fundamentals magnetic behavior quantification, thermal gravimetric analysis (TGA), and Mössbauer spectrometry. TGA and Mössbauer spectrometry also provide the dispersion quality, particle size and magnetic relaxation times and core/surface magnetic property variations for particles respectively.

1.5. Biomedical application of magnetic nanoparticles

Superparamagnetic nanoparticles have a high potential for several biomedical applications based on their physical and chemical properties. They are a potential candidate to be used in (a) drug delivery, (b) tissue repair, (d) detoxification of biological fluids, (e) hyperthermia (f) magnetic resonance imaging (MRI) [1-7]. The particles must show a high magnetic saturation, biocompatibility and a functional surface in order to be considered a good

candidate for above applications. The surfaces of these particles could be modified through organic or non-organic molecules [50]. It is also been reported that the surface of magnetic nanoparticles have been modified through oxide layers (e.g. silica or alumina) in some cases [50]. These modifications are suitable to further be functionalized by the attachment of various bioactive molecules such as peptides, antibodies, drugs, etc. As the magnetic particles accumulate to the site of action, they can play an important role in functional validation through MRI by enhancing the magnetic flux at that site to locate and measure the targeting ability of a drug carrier. In all cases, superparamagnetic particles are of interest because they do not retain any magnetism after removal of the magnetic field [51]. The effectiveness of the particles as MRI contrast agents depends upon (a) high magnetic susceptibility in order to have an effective magnetic enrichment, [52] (b) size and size distribution of particles, (c) superparamagnetic behavior, and (d) ability of the surface to further be modified for specific biomedical applications [47]. Varanda et al. have reported a linear correlation between saturation magnetization and particle size, suggesting that shape and surface curvature of nanoparticles can have an effect on magnetic properties [53]. Studies show that following systemic administration, larger particles with diameters greater than 200 nm are usually taken up by macrophages resulting in decreased blood circulation time; and particles with diameters of less than 10 nm are rapidly removed through renal clearance. This

suggests particles ranging from 10 to 200 nm are desirable for intravenous injection since they have the most prolonged blood circulation times [54].

1.5.1. Drug delivery

Another promising application of magnetic nanoparticles is in drug delivery [1]. Surface modified magnetic nanoparticles can be employed as a drug carrier for site-specific delivery of drugs (Fig 4). As the magnetic particles traverse the target organ capillaries, an applied external magnetic field may retain these particles at the desired site. Retained particles may undergo extravasation, which could ultimately lead to intracellular (i.e., tumor cell) drug uptake. Several studies demonstrated that biodegradable polymers are ideal candidates for drug carriers since they show minimum toxicity and immunological response [55, 56] . The potential advantage of a magnetically guided drug delivery system is reduced drug doses and potential side effects to healthy tissues. It has also been reported that PEG-coated superparamagnetic nanoparticles did not affect cell adhesion behavior or morphology after incubation with immortalized fibroblasts [1]. Particle size and charge along with surface must be modified to enhance their blood circulation time as well as bioavailability of the particles within the body [57]. In addition, magnetic properties and cellular internalization of particles strongly depends on the size and size distribution of the magnetic nanoparticles [58].

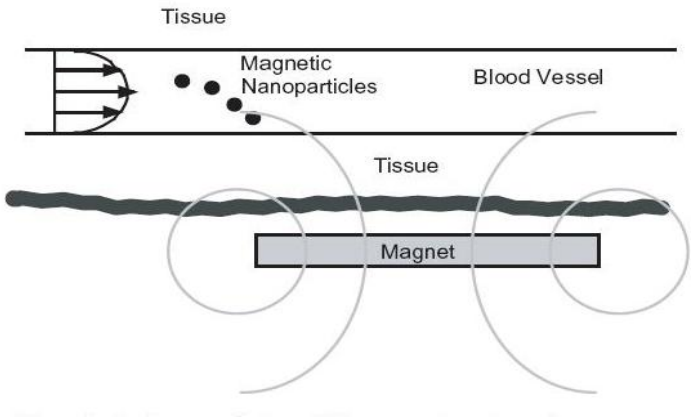

Fig 3. Magnetic nanoparticles as drug carrier vehicles.

Superparamagnetic iron oxide nanoparticles of narrow size range are easily produced and stabilized with various polymeric and non-polymeric coating since they are likely to be taken up by the body's reticuloendothelial system (RES) due to their hydrophobic surface [59]. Zhang et al. has reported PEG modified superparamagnetic iron oxide nanoparticles that have a good biocompatibility and relatively long circulation time [60]. They have shown that the amount of PEG-modified nanoparticles phagocytosed into mouse macrophage cells was much lower than that of unmodified nanoparticles. Fine ferromagnetic particles coated with poly (ethylene glycol) terminated with amino or carboxyl groups have been fabricated to further be functionalized via the covalent attachment of proteins, glycoproteins, and other ligands [61]. Because these particles are sufficiently small, they are able to reach the site of action, prior to systemic clearance. Freeman and Geer have reported that iron particles could pass through capillaries when properly conditioned [62, 63]. Ferromagnetic particles have also been used for various *in vivo* applications such as a tracer of

the blood flow. Zimmermann et al. proposed the application of erythrocytes or lymphocytes containing fine ferromagnetic particles to a desired site by an external magnetic field [61]. Interest also recently focused on core-shell magnetite particles with a shell of poly(lactide-co-glycolide).

1.5.2. Magnetic resonance imaging

MRI is a medical imaging method used to obtain images of the body in thin slices [64]. When a strong external magnetic field is applied to the body, a hydrogen nucleus in water aligns itself in the applied field direction. MRI then measures the characteristics of hydrogen nuclei of water after a radio wave is applied to push some of these protons out of alignment. Since protons in different tissues of the body (fat, muscle, etc.) re-align at different speeds, the different structures of the body can be revealed [65]. MRI gives spatial distribution of the intensity of water proton signals in the volume of the body. The signal intensity in MRI depends on the amount of water in the given place and on the magnetic relaxation times T_1 (longitudinal relaxation time) and T_2 (transverse relaxation time).

The net magnetization vector is made up of a longitudinal magnetization vector and a transverse magnetization vector. The longitudinal relaxation time (T_1) is the time required for the z-component of the magnetization vector to return to its thermal equilibrium state and the transverse relaxation time (T_2) is the time required for the component of magnetization vector perpendicular to the magnetic field to return to its thermal equilibrium state. Reducing these factors in

each case is the ultimate goal in most MRI studies. Improving the final results from MRI is only possible when the factors that have the most effect on the MRI signal intensity are altered. These factors are the amount of water in a given place and the magnetic relaxation times, T_1 and T_2. Since it is hard to influence the water intensity in specific tissue in the body, the most effective way to improve the signal intensity is through the alteration of the magnetic relaxation times T_1 and T_2 of the protons in tissue-contained water.

Application of contrast enhancers are known to change tissue characteristics and hence the MRI scan results [66]. Longitudinal relaxation time T_1 and transverse relaxation time T_2 show remarkably different behavior in the presence of paramagnetic species. The resulting effects seen in NMR spectroscopy have proven the shortening of both T_1 and T_2 in the presence of paramagnetic species used as contrast agents. Shortening of T_1 leads to an increase in signal intensity, and shortening of T_2 produces broader lines with decreased intensity [67]. The net result is a nonlinear relationship between the concentration of the contrast agent and the signal intensity. At low concentration before reaching the optimal concentration, an increase in contrast agent provides an increase in signal intensity due to the effect on T_1. Further increase in concentration reduces the signal because of the effect on T_2. This dictates the use of contrast agents with a relatively greater effect on T_1 than on T_2.

Materials with unpaired electrons, so-called “paramagnetic” species, are known to have significant effect on T_1 and T_2 relaxation time. This effect strongly

depends on the number of unpaired electrons in these species. Investigations have focused on the development of stable paramagnetic metal ion complexes using a metal chelating agent. In most cases both the metal ion and the chelating agent exhibit substantial toxicity in the unbound state. However, they usually create a less toxic, thermodynamically and kinetically stable compound when they are bound. Studies have also shown that complexation of the metal ion with organic ligand, might alter paramagnetic properties of the metal while significantly decreasing the toxicity effect. Gadolinium-DTPA complex is an FDA approved contrast agent for use in disease diagnostics. This complex is usually eliminated through the kidney. Recently, there have been concerns about the toxicity of this material in persons with impaired kidney function. Another, relatively new type of paramagnetic contrast agent is superparamagnetic iron oxide (SPIO) based colloids. They consist of non-stoichiometric microcrystalline magnetite nanoparticles mostly stabilized through polymer coatings. These colloids are currently being used as tissue specific contrast agents and studies on improvement of these contrast agents are a well-established area of pharmaceutical research. The two most widely used contrast agents for MRI scanning are gadolinium-based agents, which are T_1 contrast agents that cause positive contrast enhancement and provide brighter images upon accumulation in the target site, and superparamagnetic iron oxide particles, which are T_2 contrast agents that give negative contrast enhancement and thus darker images in areas of accumulation.

1.5.3.1. Gd (III) based contrast agents

The significant feature of Gadolinium (III) is the high number of unpaired electrons, seven. Even after binding to an organic ligand, The Gd^{3+} ion retains a number of unpaired spins. The free Gd^{3+} ion is extremely toxic, but there are a number of its complexes that are very stable and thus exhibit much less toxicity. Slow clearance from the body seems to be a problem that can significantly increase the toxicity of any Gd^{3+} complex. Covalently coupling the ligand to a protein to generate tissue-specific contrast agents is considered a potential improvement of Gd-based contrast agents. Gd-based contrast agent complexes may not be the best choice as of today because of their recently reported toxicity effect, but it is a relatively well-known choice, widely used in many MRI facilities on a daily basis [68].

1.5.3.2. Superparamagnetic iron oxide-based contrast agents

Superparamagnetic iron oxide nanoparticles are known to have a much larger effect on relaxation time compared with paramagnetic materials. Because of their single domain structure, the entire moments within the crystal structure align in the direction of the magnetic field when placed in an external field and enhance the magnetic flux. These particles do not retain any magnetization after the removal of the external field. This ability to disturb the local magnetic field through large magnetic moments leads to a rapid change in coherence of surrounding protons called dephasing, hence resulting in a detectable change in

the MR signal through altering longitudinal and transverse relaxation of the surrounding water nuclei. This implies that the imaging capability provided is not from the superparamagnetic iron oxide particles themselves but through their influence on T_1 and T_2 of water. Although the superparamagnetic nanoparticles are well known for generating a good MR contrast because of their ability to significantly reduce the transverse relaxation T_2 time, it has also been demonstrated that these particles can generate sufficient T_1 contrast for biomedical applications as well [69, 70].

Stabilized superparamagnetic iron oxide nanoparticles are promising contrast agents since their properties can be further modified for the specific application. They are relatively non-toxic and rapidly cleared from the organism. After the external magnetic field is removed, Brownian motion is sufficient to randomize the superparamagnetic nanoparticle orientation, thus leaving no magnetization.

Superparamagnetic iron oxide nanoparticles are finding applications in biomedical research. For example, Zhao et al. has used magnetic nanoparticles to detect apoptosis [71]. Apoptosis is an active process of cellular self-destruction that plays an important role in number of disorders including neurodegenerative diseases [72]. Superparamagnetic iron oxide nanoparticles are currently being used as a clinical contrast agent for MRI under the names of Lumirem, Gastromark, Ferumoxsil, Abdoscan, Feridex, Endorem and Ferumoxide. Table 2

shows some of magnetic nanoparticles that have served as MRI contrast enhancing agents in past two decades.

Table 2. Reported nanoparticle-based MRI contrast agents.

Name	Size (nm)	Coating material	References
AMI-25 (Feridex; Endorem)	80-150	Dextran	[73]
SHU 555A (Resovist)	Ca. 62	Carbodextran	[74]
AMI-227 (Combidex; Sinerem)	20-40	Dextran	[75]
CLIO; MION	10-30	Dextran	[69]

1.6. Toxicity Consideration

Studies have shown that iron oxide nanoparticles require a biocompatible sheath to prevent agglomeration that may lead to toxicity in biological media [76]. The diameter and surface characteristics of the superparamagnetic iron oxide nanoparticles play an important role in their clearance rate, cell toxicity and the cellular response to these nanoparticles. In general, nanoparticles with diameters above 200 nm are more likely to be taken up by macrophages. On the other hand, small particles with diameters less than 10 nm are removed rapidly through extravasation and renal clearance [1]. This indicates that the particle size between 10-200 nm offers the best chance to stay in circulation for a longer time. In order to prevent a toxic interaction of superparamagnetic iron oxide nanoparticles and to prolong plasma half-life of these nanoparticles, amphiphilic

coatings are introduced to extend their circulation time from minutes to hours, thereby increasing the targeting potential of a surface-modified contrast agent [77].

To date, studies have shown that the polymer-coated nanoparticles have minimal impact on cell viability and function. Gomez-Lopera et al. have fabricated magnetic nanoparticles stabilized with a biodegradable poly (DL-lactide) polymer coating [63]. The aim of their work was to synthesize colloidal particles that were both magnetic field responsive and useful as drug delivery systems. Another study shows that dextran-coated superparamagnetic nanoparticles labeled with the a cationic peptide had no significant effect on cell viability or the biodistribution of human hematopoietic cells [39]. In summary, all studies have shown that superparamagnetic iron oxide nanoparticles surface properties can influence the uptake of nanoparticles by phagocytic cells. For example, carboxydextran-coated superparamagnetic iron oxide nanoparticles appear to be internalized by macrophages to a greater extent than dextran-coated superparamagnetic iron oxide nanoparticles [78]. The most common reactions following the administration of superparamagnetic iron oxide nanoparticles are headache, back pain, vasodilatation, and hives [8].

Chapter 2

Polymer Stabilized Iron Oxide Nanoparticles

Introduction

Magnetic nanoparticles have been intensively studied for their applications in biomedical areas such as enzyme and protein immobilization, targeted drug delivery, *in vitro* cell separation and magnetic resonance (MR) contrast enhancement [1-7]. Several investigations have been carried out in the field of superparamagnetic iron oxide nanoparticles because of their high magnetic susceptibility and relatively low cytotoxicy [8]. Superparamagnetic nanoparticles possess an advantage in that they do not retain any magnetism after removal of an external magnetic field [12]. A recurrent problem with these particles, however, is that the formation of agglomerates in biological fluids is common. These agglomerates are subject to clearance and rapid biodegradation by the reticuloendothelial system [13, 14]. Agglomeration may also lead to unwanted occusions upon injection.

Researchers have been studying different techniques to overcome these difficulties by engineering the surface of iron oxide nanoparticles. To enable these nanoparticles for biomedical applications, substances that make them stable, biodegradable must be implemented colloidally. Also desirable is the ability to attach complex biological molecules, such as peptides, hormones, vitamins or drugs [16-19]. Finally, magnetic nanoparticles are desired to have a hydrophilic surface and size less than 200 nm for biomedical applications.

Several methods have been reported for surface modification of superparamagnetic iron oxide nanoparticles. Surface protection using a non-

polymeric organic layer, like oleic acid, or small “monomeric” organic molecules, have been developed as a method to stabilize magnetic nanoparticles [48]. Several synthetic and natural polymers have also been reported to modify the surface of superparamagnetic nanoparticles to enhance their function *in vivo*. These techniques often resulted in the formation of iron oxide nanoparticles with a wide particle size distribution and poor crystallinity [34]. Moreover, many of these polymer stabilizers lack a functional component to bind to the magnetite surface which decreases their long-term dispersion stability.

This dissertation reports a novel approach to synthesize iron oxide within polyvinylamine (PVAm) nanoparticles. PVAm is a water soluble polymer with a relatively high density of reactive amino groups [20]. It has been utilized as a chelating agent for heavy metals due to the presence of primary amine side-groups along the polymeric backbone [21]. The resulting PVAm nanoparticles containing iron oxide were dispersible in water and stable at biological pH (7.4). A relatively high density of reactive amino groups on the surface of these nanoparticles may enable them to functionalization for targeted imaging or drug delivery.

2. Materials and Methods

2.1. Materials

N-vinylformamide (NVF; Aldrich) was used as a monomer and 2, 2’-Azobis(2,4-dimethylpentanitrile) (Vazo-52, purchased from DuPont) used as an initiator for

the polymerization reaction of N-vinylformamide. Vazo-52 has 10 hr half life at 52 °C which makes it a good candidate for reaction polymerization at low temparutures.. Deionized water (DI) was obtained from a Barnstead EasyPure water purifier. All materials were used as received.

2.2. Synthesis of Non-Degradable Cross-Linker

NVEE was synthesized following the procedure reported in appendix *I*. NVEE is a NVF derivative, which makes it a good candidate for co-polymerization with NVF.

2.3. Synthesis of Poly (N-vinyl Formamide) Nanoparticles

Cross-linked PNVF nanoparticles were fabricated by inverse microemulsion polymerization of NVF with NVEE. NVF (350 µL) was added to 20 mg of initiator and stirred, then 50 mg of NVEE and 165 µL of DI water were added to this solution, respectively. The resulting transparent solution was next added to 100 mL hexane containing 30 mg of initiator, Tween 80 (3 g) and Span 80 (4.1 g) under vigorous stirring. In the next step, the microemulsion was transferred into a 150 mL jacketed three-neck reactor. Before the polymerization reaction started, nitrogen was sprayed for 15 minutes to remove oxygen. The polymerization reaction was then carried out at 50ºC for 24 hours. PNVF nanoparticles were purified by centrifugation at 15,000 rpm for 45 minutes at room temperature. The particles then were re-dispersed in DI water and dialyzed against DI water for two

days. To optimize the final size of PNVF nanoparticles several experiments were performed. Appendix *II* shows the optimization results.

2.4. Synthesis of Polyvinylamine Nanoparticles

PVAm nanoparticles were produced by subsequently hydrolyzing the PNVF particles (Fig. 4).

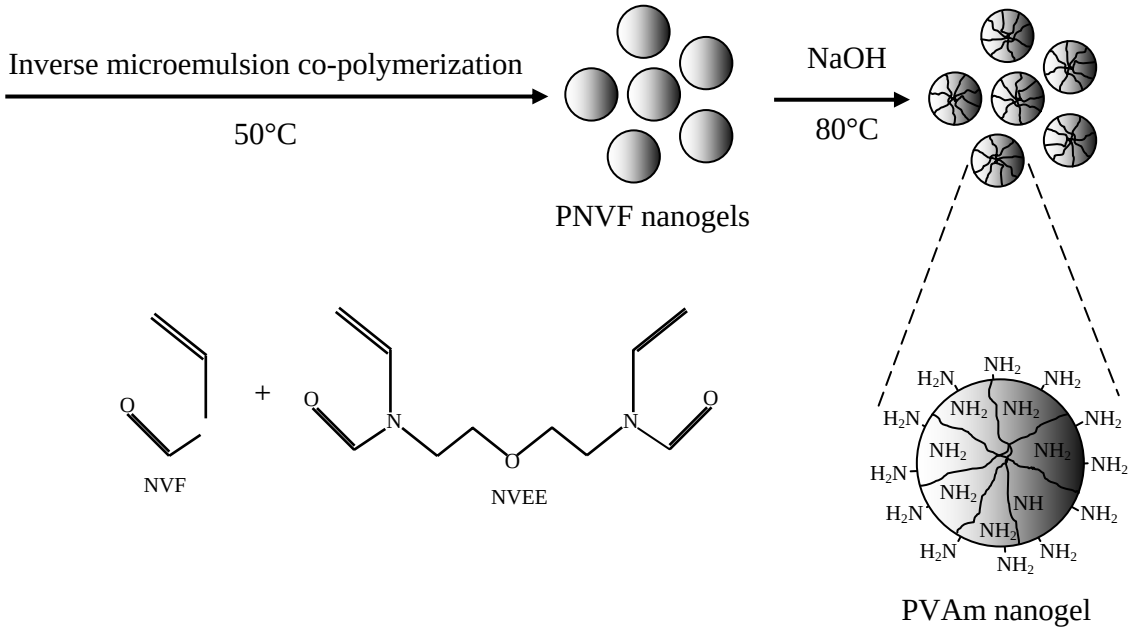

Figure 4. Synthesis of cross-linked polyvinylamine nanoparticles.

1M NaOH solution was prepared by dissolving 1.2 g NaOH in 30 mL PNVF suspension (~5 mg/mL) and stirred under nitrogen. The resulting solution was then incubated at 80°C for 12 hours. The PVAm nanoparticles obtained from this process were purified by dialysis against water for 5 hours. This procedure resulted in the production of PVAm nanoparticles. The amount of formamide

group converted amine group can be measured using NMR spectra [79]. The effect of hydrolysis time on PVAm size and charge was also studied. Hydrolyzed nanoparticles contained amine functional groups both inside and at the surface.

2.5. Fabrication of Magnetic Polyvinylamine Nanoparticles

To synthesize the iron oxide inside the PVAm nanoparticles, the following reaction should be performed in aqueous solution using a molar ratio of Fe (II) / Fe (III) = 0.5 [80] .

$$FeCl_2 + 2FeCl_3 \rightarrow Fe_3O_4$$

$FeCl_2$ (4 g) and $FeCl_3$ (5.2 g) were successively dissolved in 25 mL of deoxygenated PVAm nanoparticle suspension (5 mg/mL). This mass ratio was determined experimentally to yield roughly a 0.5 ratio within nanoparticles [22]. The solution was stirred over night at room temperature.

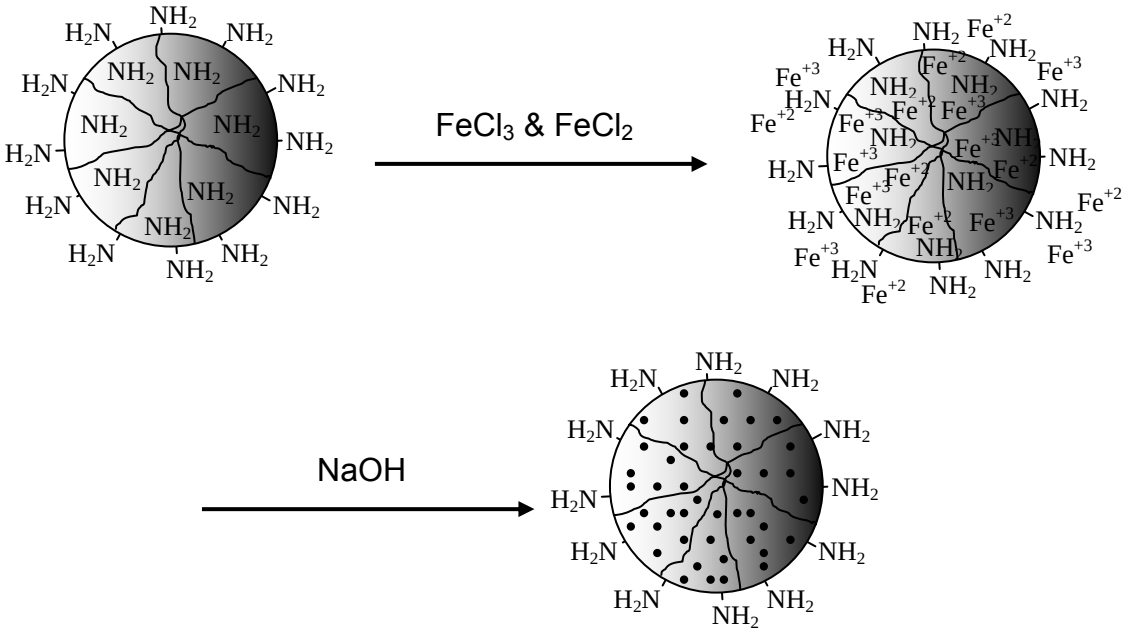

Figure 5. Synthesis of magnetic PVAm nanoparticles. Amine functional groups chelate iron ions inside and on the surface of the polymeric matrix. Black dots depict the iron oxide inside the polymeric matrix after oxidation.

Next the solution of PVAm nanoparticles containing $FeCl_2$ and $FeCl_3$ was transferred to a centrifuge tube and centrifuged for 30 minutes at 15,000 rpm. The pellet was re-dispersed in deoxygenized water and the supernatant was stored to further study the iron uptake by PVAm nanoparticles. The resulting solution was added drop-wise into 50 mL of 1 M NaOH solution under vigorous stirring. The last step generated a black-brown precipitate almost instantly. The precipitate was isolated using a magnetic field and the supernatant was removed from the precipitate by decantation. Deoxygenated water was then added to the easily redispersed precipitate and the solution was centrifuged at 15,000 rpm for 30 minutes. HCl (0.1 M) solution was added to the precipitate under stirring to re-disperse the magnetic pellet in centrifuge tubes. The resulting opaque solution then was washed with PBS with pH > 9 and then with PBS (pH 7.4).

2.6. Characterization

2.6.1. Size, Size Distribution and Charge Characterization of PVAm and Magnetic PVAm Nanoparticles

2.6.1.1. Transmission electron microscopy studies

The size and morphology of magnetic nanoparticles were observed by transmission electron microscopy (JEOL 1200 EXII) at 200 Kv. In addition, energy dispersive X-ray spectroscopy (EDX) was used to qualify the iron oxide in PVAm nanoparticles. The powder was dissolved in water and was drop-cast onto a 300 mesh carbon-coated copper grid that was air dried before imaging.

2.6.1.2. Dynamic light scattering studies

The size, size distribution and the zeta potential of PVAm nanoparticles and PVAm nanoparticles containing iron oxide dispersed in PBS (pH=7.4) were measured by dynamic light scattering (Brookhaven Zeta-PALS). Samples were diluted prior to the measurements. The zeta potential was determined in the presence of 0.1 M KCl solution to maintain the ionic strength required for the measurement. Polydispersity was determined according to the method of cumulants [81].

2.6.2. Characterization of Magnetic PVAm Nanoparticles

2.6.2.1. Iron Content Measurement

2.6.2.1.1. Iron Uptake

To determine the molar ratio Fe (II) / Fe (III) inside polymeric nanoparticles, UV absorbance spectra were obtained to study the amount of iron ions coordinated by PVAm nanoparticles performing the following protocol. Reagent A was made by adding 0.25 g ferrozin to 0.401 g ammonium acetate and diluted to 50 mL. Hydroxylamine HCL (1.4 mmol/L) in 2 mol/L HCL and 10 mol/L ammonium acetate adjusted to pH 9.5 with ammonium hydroxide were used as reagent B and C respectively. Standard curve was made using ferrous ammonium sulphate and water to make serial dilutions. To find the Fe (II) concentration, UV samples were prepared by adding 3 mL H_2O to 100 µL of sample, then 100 µL of reagent was added to the solution and kept for 10 minutes at room temperature. The absorbance then was measured at 562 nm. Next, 1 mL of the above mixture was added to 150 µL of reagent B where it was mixed and allowed to stand overnight to reduce Fe (III) to Fe (II), then 50 µL of reagent C was added and the solution was kept for 10 minutes at room temperature. UV spectra were recorded at the same wavelength to measure the concentration of Fe (II).

2.6.2.1.2. Final Iron content

The content of Fe_3O_4 in magnetic polymeric particles was measured by atomic absorption spectroscopy (AA). The suspension of magnetic PVAm was diluted with HCL (2% V/V). The instrument used was a Perkin Elmer AAnalyst 300 with a AS90 plus auto sampler. A regular sensitivity nebulizer without an impact bead

was installed as well as a 10 cm single slot burner head. The bulb was a Perkin Elmer Fe bulb.

2.6.2.2. Magnetic measurements

The magnetization curves of PVAm nanoparticles containing iron oxide were carried out at room temperature (magnetic field between -20 and 20 kOe) using a Quantum Design MPMS 5 superconducting quantum interface device (SQUID) magnetometer. Mass magnetization is defined as the magnetic moment per total mass of the sample.

2.6.2.3. Fourier Transform Infrared Spectroscopy Studies

The Fourier transform infrared (FTIR) spectra of the sample were recorded on a MAGNA-IR 560 spectrometer. The freeze-dried samples (2 mg) of pure PVAm (5 mg/mL) and PVAm containing iron oxide (6.5 mg/mL) were ground with KBr, and the mixture was compressed into a pellet. The spectrum was taken from 3999 to 500 cm^{-1} (4 cm^{-1} resolution, 32 scans).

2.6.2.4. In vitro Cytotoxicity Studies

To test whether the PVAm nanoparticles containing iron oxide have biocompatibility, a cytotoxicity assay was performed. A549 cells were trypsinized, counted and diluted to a concentration of approximately 80,000 cells/mL. Then 0.1 mL was added to each well of a 96-well plate and the cells were incubated in

5% CO_2 incubator at 37°C for 24 hours. Medium were then removed and replaced with a mixture of 100 µL fresh culture medium and 20 µL MTS reagent solution. The cells were incubated for 3 hours at 37°C in the 5% CO_2 incubator. The absorbance of each well was then measured at 490 nm to determine cell viability.

2.7. Results and Discussion.

2.7.1. Size and charge characterization of PVAm and magnetic PVAm Nanoparticles.

2.7.1.1. Dynamic Light Scattering

The presence of reactive amine groups along with the hydrophilicity of PNVF and PVAm made this polymer an attractive candidate for incorporating iron oxide into nanoparticles. Methods were developed to determine reaction conditions that provided the desired particle size and size distributions of both PVAm and magnetic PVAm nanoparticles. Hydrolysis time showed a significant effect on PVAm size and charge. The size of PVAm nanoparticles increased with increasing time (Fig. 6A). Zeta potential of PVAm nanoparticles also increased over time (Fig. 6B). It is hypothesized that the increased particle charge resulted in an increase in osmotic pressure due to increased concentration within the nanoparticles [82].

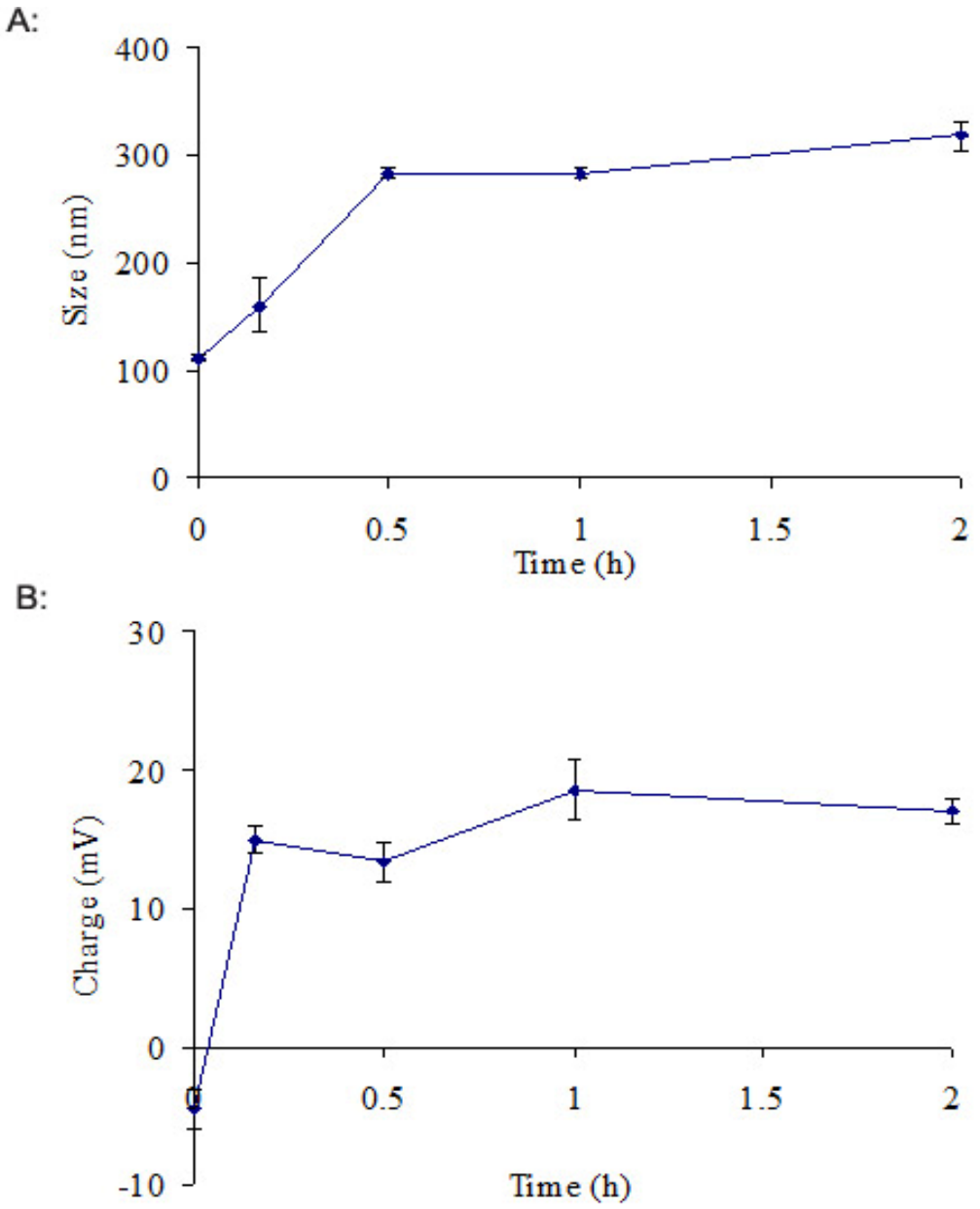

Figure 6. PVAm (A) size and (B) charge increases with hydrolysis time during the conversion of PNVF to PVAm.

In general, in polyelectrolyte gels there is a difference in mobile ion concentrations inside and outside the gel. This difference is caused by the requirement to satisfy electroneutrality and leads to an osmotic pressure

difference between the gel and the equilibrium solution. Table 3 shows the size and zeta potential of nanoparticles that were used to fabricate magnetic PVAm nanoparticles. The PNVF nanoparticles were hydrolyzed for 20 minutes to obtain particles with the specified size and charge.

Table 3. Characteristics of synthesized nanoparticles.

	Nanoparticle Diameter (nm)	Polydispersity	Zeta Potential (mV)
PNVF	112 ± 13	0.182 ± 0.089	-5.6 ± 0.3
PVAm	186 ± 3	0.159 ± 0.002	23.9 ± 2.6
Magnetic PVAm	155 ± 5	0.146 ± 0.003	15.5 ± 0.1

Magnetic nanoparticle size and size distributions were also studied. Dynamic light scattering studies further confirmed that PVAm and magnetic PVAm nanoparticles had low polydispersity. In most cases, particles with a polydispersity < 0.2 are considered narrowly dispersed (Table 3).

2.7.1.2. Transmission Electron Microscopy

Transmission electron microscopy (TEM) was used to probe PNVF, PVAm and magnetic PVAm nanoparticle morphology. Images from TEM indicated that PNVF (Fig. 7A), PVAm (Fig. 7B) and magnetic PVAm nanoparticles (Fig. 7C & 7D) were spherical with a ruffled surface. The ruffled surface morphology was expected since nanoparticles must be imaged in a dry state when using TEM.

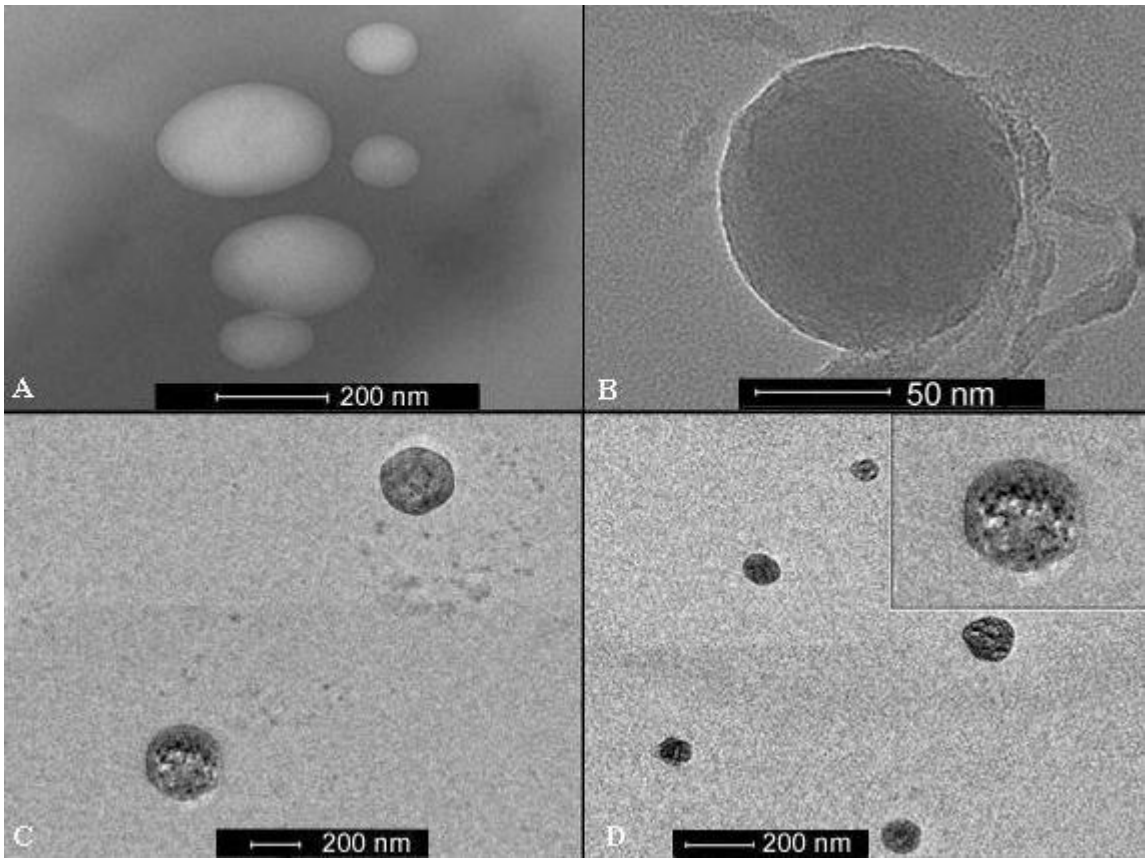

Figure 7. TEM analysis showed that (A) PNVF, (B) PVAm, and (C & D) magnetic PVAm nanoparticles were spherical. In addition, small iron oxide nanoparticles (<10 nm) were evident within magnetic PVAm nanoparticles.

TEM was also used to detect the iron oxide inside nanoparticles (Fig. 7C & 7D). The dark spots inside the nanoparticles along with the energy dispersive X-ray spectroscopy (EDX) data of the same magnetic particles (Fig. 8) indicated the presence of small iron oxide nanoparticles (<10 nm) inside the PVAm nanoparticles. Characteristics X-Rays results from non-radiative transition of electron between shells within a, K, L or M family of an atom. K lines are the most energetic lines consisting of $K\alpha_1$, $K\alpha_2$, $K\beta_1$, and $K\beta_2$ radiations. Other

researchers have reported similar morphology of magnetic nanoparticles [83, 84]. Image analysis software determined that dried PVAm and magnetic PVAm nanoparticles were roughly 100 nm.

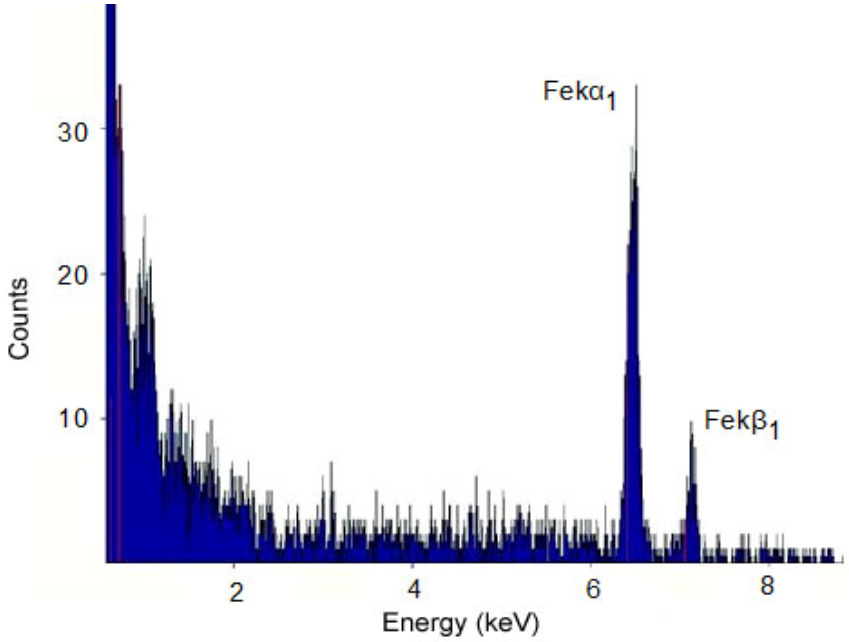

Figure 8. EDX of magnetic PVAm nanoparticles revealed two iron peaks that indicated the presence of iron inside the nanoparticles.

Comparing with the reported method for preparing stable iron oxide nanoparticles, the synthetic procedure reported here was simple since stabilization was accomplished during the iron oxide synthesis and the final product did not require any further size-selection process. Zaitsev et al. have reported the *in situ* preparation of magnetic nanoparticles by addition of a magnetite nanoparticle dispersion to the seed precipitation polymerization of methacrylic acid and hydroxyethyl methacrylate monomers [85]. The magnetite

and the polymer coated magnetite nanoparticles were reported to be ~6 - 80 nm and 340 - 400 nm in diameter, respectively. In another study, Arias et al. have reported polymer coated particles ~144 nm in diameter with ~84 nm magnetic cores [86]. The stabilized magnetic PVAm nanoparticles reported here are larger than polymer stabilized iron oxide systems previously reported. The iron oxide nanoparticles formed within PVAm nanoparticles, however, were <10 nm in diameter. Iron oxide particles formed in the presence of dextran and polyvinyl alcohol were similar in size; 4.11 ± 0.85 nm and 5.78 ± 1.30 nm, respectively [87].

2.7.2. Characterization of magnetic PVAm Nanoparticles.

2.7.2.1. Quantification of Iron Oxide Fabricated in Polyvinylamine Nanoparticles (UV)

A UV study was used to quantify the uptake of iron ions by PVAm nanoparticles (Table 4). To maintain the stochiometric molar ratio of Fe (II) / Fe (III) inside the particle, two different molar ratios of iron chloride II and III were added to the PVAm nanoparticle suspension. The amount of free iron ions was then found using UV analysis. Results indicated that the uptake of Fe (II) at low concentration (0.08 g/mL) is 47% lower than its uptake at higher concentration (0.16 g/mL). It is hypothesized that the larger electrostatic/ionic interaction between Fe (III) and amine groups relative to Fe (II) could be a reason for the higher uptake of Fe (III) ions by PVAm at low concentrations. One should

consider the concentration of amine groups inside PVAm nanoparticle, which may have a significant affect on the uptake of iron ions.

Table 4. Iron uptake by PVAm nanoparticles.

Fe(II)/Fe(III) added to PVAm solution	Fe(II)/Fe(III) inside particle	%Fe(II) uptake by particle	%Fe(III) uptake by particle	%Total uptake of iron	% Iron oxide after purification (AA)
0.50	0.15	37	93	77	10 ± 0.13
1	0.43	55	96	78	12 ± 0.01

2.7.2.1. Quantification of Iron Oxide Fabricated in Polyvinylamine Nanoparticles (AA)

Atomic absorption spectroscopy (AA) of purified magnetic nanoparticles demonstrated that the magnetite concentration in PVAm particles was ~12% (wt/wt). Data from the UV study using an indirect quantification method suggested that the total magnetite concentration inside polymer particles was of 78% (wt/wt), which was significantly higher than the 12% wt/wt detected using AA. This means that some iron ions were lost during washing or iron oxide nanoparticles formed during oxidation have been removed during purification. Gupta et al. have reported the total of particles presented in one gram of PEG modified iron oxide nanoparticles to be 1.71×10^{17} [1]. A total of 1.073×10^{22} iron particles were present in one gram of PVAm nanoparticles containing iron oxide which is higher than the amount reported for PEG-modified iron oxide nanoparticles.

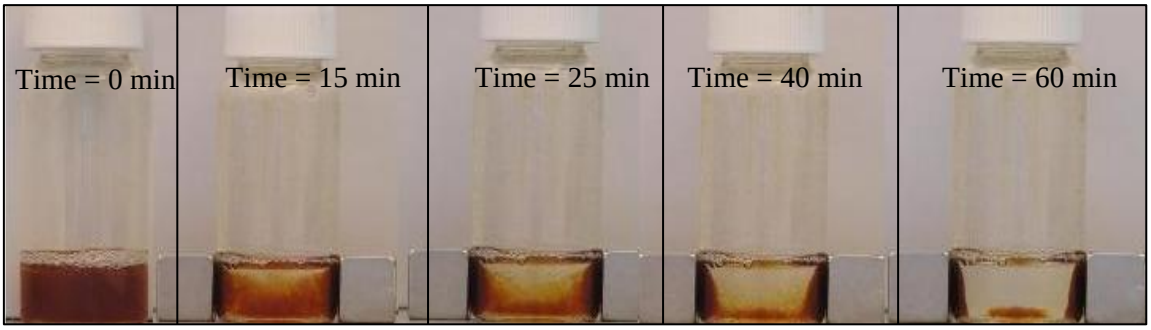

Figure 9. Magnetic PVAm nanoparticles isolated under a magnetic field.

The synthesized PVAm superparamagnetic nanoparticles were well dispersed in water and showed magnetic properties upon applying a magnetic field (Fig. 9). Particles concentrated by the magnetic field were readily redispersible. These results suggested that the magnetic PVAm nanoparticles offer colloidal stability without agglomeration.

2.7.2.2. Magnetization Results

The relative magnetization curves were determined as a function of magnetic field strength for magnetic PVAm nanoparticles (Fig. 10A). The magnetic PVAm nanoparticles were characterized by a high magnetic moment in a high magnetic field (generally, about 5 to 90 emu/g of metal oxide). The magnetic moment in the absence of an applied field was subtracted from the result. The magnetization curve exhibits zero magnetization upon the removal of magnetic field, which is a characteristic behavior of superparamagnetic particles. This

indicates that the iron oxide incorporated in nanoparticles corresponds to the single-crystal domain, exhibiting only one orientation of magnetic moment.

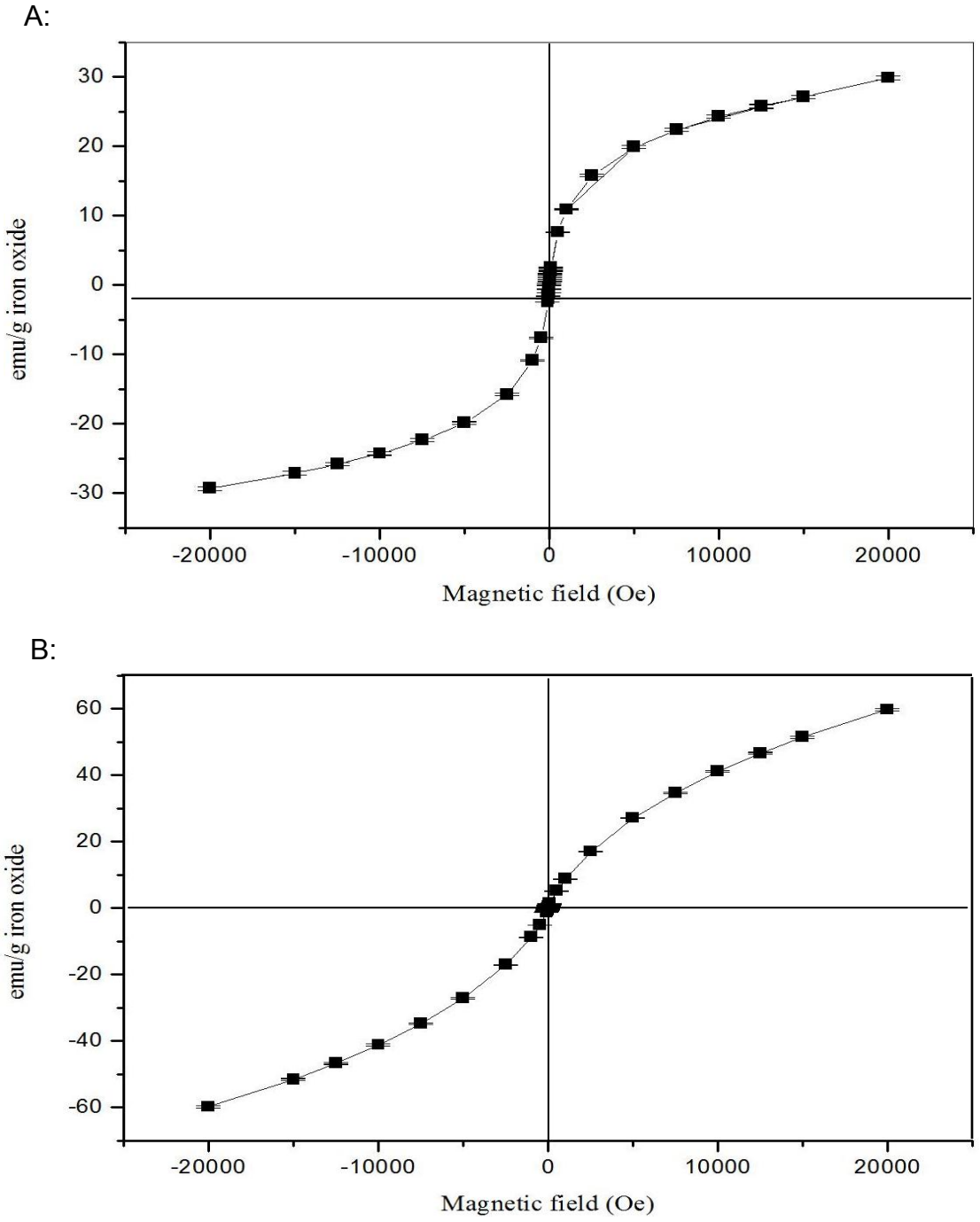

Figure 10. (A) Magnetization vs. applied magnetic filed for ~150 nm and (B) ~ 500 nm magnetic PVAm nanoparticles at room temperature.

The saturation magnetization of the ≈150 nm magnetic PVAm nanoparticles was 30 emu/g. In addition, Selim et al. have reported saturation magnetization of lactobionic acid (LA) modified iron oxide to be about 20 emu/g [88]. Their result proved that LA modified nanoparticles with saturation magnetization about 20 emu/g offered potential to be used as MRI contrast agents. The high magnetization of magnetic PVAm nanoparticles makes them susceptible to the magnetic field and, therefore, they are a candidate for MRI contrast enhancement as well. The mass magnetization of particles depended on the size of the particle providing credence to literature [15]. These results showed that larger magnetic PVAm nanoparticles had greater mass magnetization (Fig. 10B). Experimental values for the saturation magnetization of magnetic nanoparticles reported for similarly sized iron oxide nanoparticles ranges from 30-60 emu/g, where the bulk magnetite saturation can be as high as is 92 emu/g [89]. The reported values for magnetic PVAm nanoparticles were lower suggesting that the amount of iron oxide incorporated inside PVAm nanoparticles is relatively low. To achieve higher saturation magnetization it may be necessary to increase the amount of iron oxide inside PVAm nanoparticles.

2.7.2.3. The Coordination of PVAm and Iron Oxide on the Preparation of Magnetic PVAm Nanoparticles

FTIE spectra were recorded to study the coordination of iron within PVAm nanoparticles .FTIR spectra of pure PVAm and magnetic PVAm nanoparticles showed that N-H absorption bands were shifted from 3271.14 to 3178.82 cm^{-1} in

the presence of iron oxide (Fig. 11). The stretching of this amine suggested that iron oxide interacted with amine groups of PVAm. The interaction between amine groups and iron molecules is expected since primary amines are known to be chelating agents for metals like iron [21] .

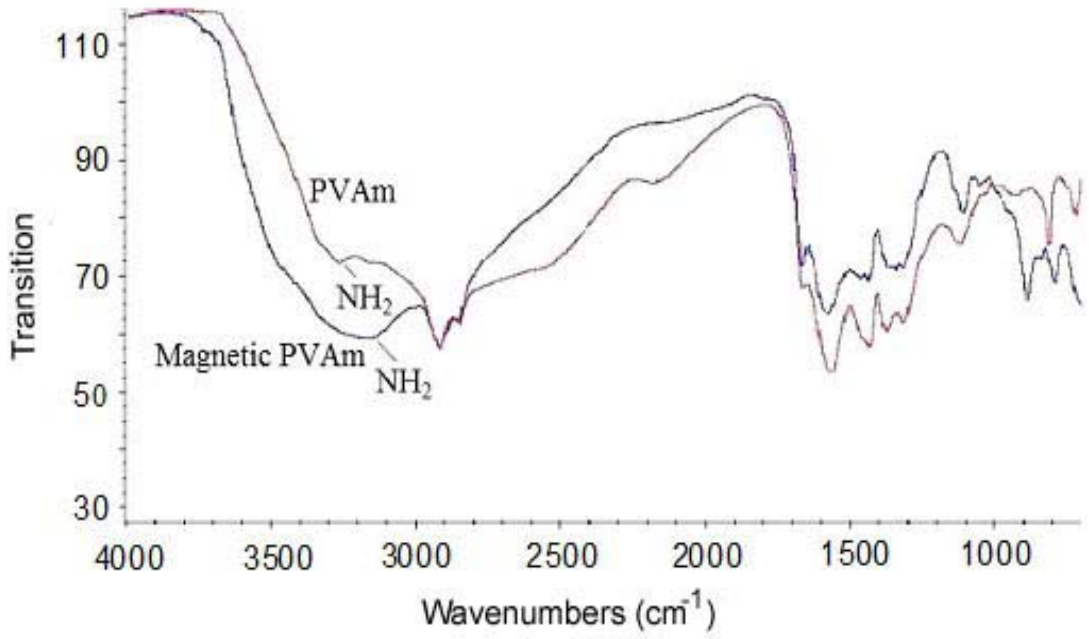

Figure 11. FTIR spectra of PVAm and magnetic PVAm nanoparticles.

2.7.2.4. Cytotoxicity Analysis

A cell proliferation assay was performed using human umbilical cord vascular endothelial cells (HUVEC) to test cell viability in the presence of PVAm and magnetic PVAm nanoparticles. The viability of the cells was determined after 24 hours. Results showed that magnetic PVAm nanoparticles have an IC_{50} > 2 mg/mL (Fig. 12). Gupta et al. has reported that PEG-coated nanoparticles showed no cytotoxic effects to cells and they remained more than 100% viable

relative to non-modified iron oxide nanoparticles at concentration as high as 1 mg/mL [1]. The toxic behavior of PVAm nanoparticles ($IC_{50} \approx 0.1$ mg/mL) is likely related to its high positive charge [90]. The increased cell viability in magnetic PVAm nanoparticles may be explained by the fact that primary amine groups in PVAm nanoparticles were occupied through association with iron ions. This interaction also decreased the zeta potential of nanoparticles from 23.9 mV to 15.5 mV.

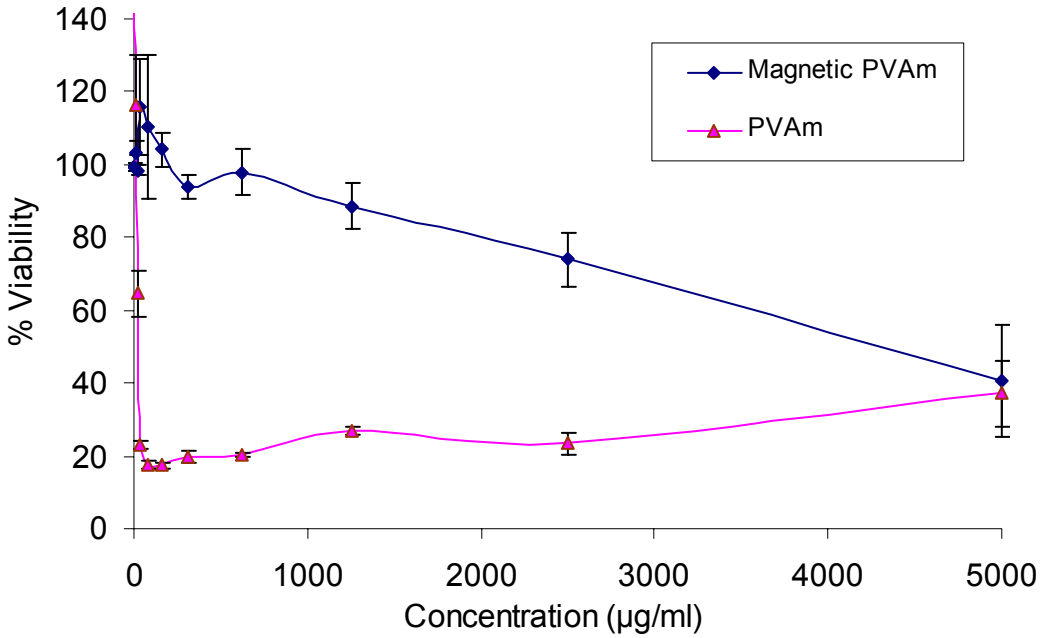

Figure10. PVAm and magnetic PVAm nanoparticles Cytotoxicity

2.8. Conclusion

In this study, magnetic PVAm nanoparticles about 150 nm in size with a very narrow size distribution have been reported. The chelating property of primary

amine functional groups in PVAm nanoparticles was suspected to hold iron ions inside the polymeric network. An oxidation reaction was then carried out inside PVAm nanoparticles to fabricate superparamagnetic iron oxide nanoparticles *in situ*. Magnetic PVAm nanoparticles were easily isolated via application of an external magnetic field and demonstrated excellent magnetic stability. Magnetic PVAm nanoparticles did not retain any magnetization upon after the removal of an external magnetic field which proved the superparamagnetic characteristic of these nanoparticles. The relatively low cytotoxicity of magnetic PVAm nanoparticles makes them a good candidate for biomedical applications. In addition, these nanoparticles possess reactive primary amines that may be modified to enable targeted delivery of this contrast enhancing agent.

2.9. Future Work

Research related to magnetic PVAm nanoparticles is of course far from closed with this thesis. Future work will aim to improve the size and charge of PVAm and magnetic PVAm nanoparticles. Future efforts can address improving the magnetization of magnetic PVAm while maintaining the size of these nanoparticles.

Next, magnetic PVAm nanoparticles will be modified to enable targeted delivery. Unbound amine groups of magnetic PVAm nanoparticles will be conjugated with ICAM-1 peptides to study their function *in vivo*. ICAM-1 peptides associate with receptors of the integrin family, thereby mediating cell-cell

interactions and allowing for signal transduction. These modified nanoparticles will later be used as MRI contrast enhancers for molecular imaging.

Polyvinyl alcohol will be synthesized as an alternative to PVAm nanoparticles. Polyvinyl alcohol is a water-soluble synthetic polymer. It is usually prepared through the removal of acetate groups of polyvinyl acetate via partial or complete hydrolysis. The polyvinyl alcohol nanoparticles can then be used to incorporate iodine. Iodine is known as a substance that enhances the contrast in X-Ray computer tomography (CT) scanning.

Later, the contrast enhancing property of the modified magnetic PVAm nanoparticles in MR imaging will be compared with the same property of polyvinyl alcohol containing iodine in X-Ray computer tomography (CT) scanning.

3. References

1. Gupta, A.K. and S. Wells, *Surface-modified superparamagnetic nanoparticles for drug delivery: preparation, characterization, and cytotoxicity studies.* NanoBioscience, IEEE Transactions on, 2004. **3**(1): p. 66-73.
2. Matsunaga, T., et al., *Chemiluminescence enzyme immunoassay using ProteinA-bacterial magnetite complex.* Journal of Magnetism and Magnetic Materials, 1999. **194**(1): p. 126-131.

3. DA, B., *Controlled biomineralization of magnetic minerals by magnetotactic bacteria.* Chem Geol, 1996. **8**: p. 132-191.

4. Taylor, J.I., et al., *Application of magnetite and silica–magnetite composites to the isolation of genomic DNA.* Journal of Chromatography A, 2000. **890**(1): p. 159-166.

5. Mornet, S., et al., *DNA–magnetite nanocomposite materials.* Materials Letters, 2000. **42**(3): p. 183-188.

6. Reetz, M.T., et al., *Entrapment of lipases in hydrophobic magnetite-containing sol-gel materials: magnetic separation of heterogeneous biocatalysts.* Journal of Molecular Catalysis. A, Chemical, 1998. **134**(1-3): p. 251-258.

7. Johnson, G.A., et al., *Histology by magnetic resonance microscopy.* Magn Reson Q, 1993. **9**(1): p. 1-30.

8. Schwertmann, U. and R.M. Cornell, *Iron oxides in the laboratory: preparation and characterization*. 2000: WILEY-VCH Verlag GMBH & Co. KGaA Weinheim, Germany.

9. Li-Ying, Z., et al., *Magnetic Behaviour and Heating Effect of Fe3O4 Ferrofluids Composed of Monodisperse Nanoparticles.* Chinese Physics Letters, 2007. **24**: p. 483-486.

10. Aime, S., et al., *Insights into the use of paramagnetic Gd (III) complexes in MR-molecular imaging investigations.* Journal of Magnetic Resonance Imaging, 2002. **16**(4): p. 394-406.

11. Lee, J.S., et al., *MR Imaging of in Vivo Recruitment of Iron Oxide-labeled Macrophages in Experimentally Induced Soft-Tissue Infection in Mice.* Radiology, 2006. **241**(1): p. 142.

12. Marc, J.M.I., et al., *Superparamagnetic Nanoparticles of Iron Oxides for Magnetic Resonance Imaging Applications.* Nanomaterials for Medical Diagnosis and Therapy, 2007.

13. Santra, S., et al., *Synthesis and characterization of silica-coated iron oxide nanoparticles in microemulsion: The effect of nonionic surfactants.* Langmuir, 2001. **17**(10): p. 2900-2906.

14. Yang, H.H., et al., *Magnetite-containing spherical silica nanoparticles for biocatalysis and bioseparations.* Anal. Chem, 2004. **76**(5): p. 1316-1321.

15. Gupta, A.K. and M. Gupta, *Synthesis and surface engineering of iron oxide nanoparticles for biomedical applications.* Biomaterials, 2005. **26**(18): p. 3995-4021.

16. Liang, Y.Y., et al., *Polysaccharide-modified iron oxide nanoparticles as an effective magnetic affinity adsorbent for bovine serum albumin.* Colloid & Polymer Science, 2007. **285**(11): p. 1193-1199.

17. Sadeghiani, N., et al., *Genotoxicity and inflammatory investigation in mice treated with magnetite nanoparticles surface coated with polyaspartic acid.* Journal of Magnetism and Magnetic Materials, 2005. **289**: p. 466-468.

18. Zhao, X. and J. Milton Harris, *Novel degradable poly (ethylene glycol) hydrogels for controlled release of protein.* Journal of Pharmaceutical Sciences, 1998. **87**(11): p. 1450-1458.

19. Shieh, D.B., et al., *Aqueous dispersions of magnetite nanoparticles with NH3+ surfaces for magnetic manipulations of biomolecules and MRI contrast agents.* Biomaterials, 2005. **26**(34): p. 7183-7191.

20. L.Gu, S.Z., A.N Hrymak, *Acidic and basic hydrolysis of Poly(N-vinylformamide).* Journal of applied polymeric science, 2002. **86**: p. 3412-3419.

21. Witek, E.W.A., *Mechanism for Base Hydrolysis of Poly (N-vinylformamide).* Journal of Macromolecular Science, Part A, 2007. **44**(5): p. 503-507.

22. Cotton FA, W.G., *Advanced inorganic chemistry*, ed. W. Interscience. 1988, New York.

23. Gupta, A.K. and A.S.G. Curtis, *Lactoferrin and ceruloplasmin derivatized superparamagnetic iron oxide nanoparticles for targeting cell surface receptors.* Biomaterials, 2004. **25**(15): p. 3029-3040.

24. Reimers, G.W., *Preparing magnetic fluids by a peptizing method.* 1972.

25. Hadjipanayis, G.C. and R.W. Siegl, *Nanophase Materials Synthesis-Properties-Applications.* 1994.

26. Rosensweig, R.E., *Ferrohydrodynamic*. 1985, Cambridge.

27. Bagwe, R.P., et al., *Improved drug delivery using microemulsions: rationale, recent progress, and new horizons.* Crit Rev Ther Drug Carrier Syst, 2001. **18**(1): p. 77-140.

28. Hochepied, J.F. and M.P. Pileni, *Magnetic properties of mixed cobalt–zinc ferrite nanoparticles.* Journal of Applied Physics, 2000. **87**: p. 2472.

29. Lawrence, M.J., *Surfactant systems: microemulsions and vesicles as vehicles for drug delivery.* Eur J Drug Metab Pharmacokinet, 1994. **19**(3): p. 257-69.

30. Portet, D., et al., *Nonpolymeric Coatings of Iron Oxide Colloids for Biological Use as Magnetic Resonance Imaging Contrast Agents.* Journal of Colloid and Interface Science, 2001. **238**(1): p. 37-42.

31. Ayyub, P., et al., *Size-induced structural phase transitions and hyperfine properties of microcrystalline Fe, O.*

32. Hamley, I.W., *Nanotechnology with Soft Materials.* Angewandte Chemie International Edition, 2003. **42**(15): p. 1692-1712.

33. Tepper, T., et al., *Magneto-optical properties of iron oxide films.* Journal of Applied Physics, 2003. **93**: p. 6948.

34. Ha Young Lee, N.H.L., 2 Jin A. Seo,, *Preparation and Magnetic Resonance Imaging Effect of plyvinylpyrrolidone-Coated Iron Oxide Nanoparticles.* Journal of biomedical materials research, 2005. **79b**(142-5).

35. Kaufman, C.L., et al., *Superparamagnetic iron oxide particles transactivator protein-fluorescein isothiocyanate particle labeling for in vivo magnetic resonance imaging detection of cell migration: uptake and durability.* Transplantation, 2003. **76**(7): p. 1043.

36. Berry, C.C., et al., *Dextran and albumin derivatised iron oxide nanoparticles: influence on fibroblasts in vitro.* Biomaterials, 2003. **24**(25): p. 4551-4557.

37. D'Souza, A.J.M., R.L. Schowen, and E.M. Topp, *Polyvinylpyrrolidone–drug conjugate: synthesis and release mechanism.* Journal of Controlled Release, 2004. **94**(1): p. 91-100.

38. Shan, G., et al., *Immobilization of Pseudomonas delafieldii with magnetic polyvinyl alcohol beads and its application in biodesulfurization.* Biotechnology Letters, 2003. **25**(23): p. 1977-1981.

39. Lewin, M., et al., *Tat peptide-derivatized magnetic nanoparticles allow in vivo tracking and recovery of progenitor cells.* Nature Biotechnology, 2000. **18**: p. 410-414.

40. Gupta, P.K. and C.T. Hung, *Magnetically controlled targeted micro-carrier systems.* Life Sci, 1989. **44**(3): p. 175-86.

41. Ugelstad, J., et al., *Monodisperse magnetic polymer particles. New biochemical and biomedical applications.* Blood Purif, 1993. **11**(6): p. 349-69.

42. Sauzedde, F., A. Elaïssari, and C. Pichot, *Hydrophilic magnetic polymer latexes. 1. Adsorption of magnetic iron oxide nanoparticles onto various cationic latexes.* Colloid & Polymer Science, 1999. **277**(9): p. 846-855.

43. Chatterjee, J., Haik, Y. and Chen, C.- J.,, *Modification and Characterization of Polystyrene Based Magnetic Microspheres and its Comparison with Albumin Based Magnetic Microspheres.* Journal of Magnetism and Magnetic Materials, 2001. **225**(21).

44. M, L.J.I.T.S., *Preparation of Ultrafine Fe3O4 Particles by Precipitation in the Presence of PVA at High pH.* Journal of Colloid and Interface Science, 1996. **177**(5): p. 490-495.

45. Ng, V., et al., *Nanostructure array fabrication with temperature-controlled self-assembly techniques.* Nanotechnology(Bristol. Print), 2002. **13**(5): p. 554-558.

46. Kataby, G., et al., *Coating of Amorphous Iron Nanoparticles by Long-Chain Alcohols.* Langmuir, 1998. **14**(7): p. 1512-1515.

47. Moghimi, S.M., A.C. Hunter, and J.C. Murray, *Long-Circulating and Target-Specific Nanoparticles: Theory to Practice.* Pharmacological Reviews, 2001. **53**(2): p. 283.

48. Tadmor, R., et al., *Resolving the puzzle of ferrofluid dispersants.* Langmuir, 2000. **16**(24): p. 9117-9120.

49. Sahoo, Y., et al., *Alkyl Phosphonate/Phosphate Coating on Magnetite Nanoparticles: A Comparison with Fatty Acids.* Superlattices Microstruct, 1996. **19**: p. 191.

50. Berry, C.C. and A.S.G. Curtis, *Functionalisation of magnetic nanoparticles for applications in biomedicine.* J. Phys. D: Appl. Phys, 2003. **36**: p. R198-R206.

51. Tartaj, P., et al., *The preparation of magnetic nanoparticles for applications in biomedicine.* J. Phys. D: Appl. Phys, 2003. **36**: p. R182-R197.

52. Jordan, A., et al., *Presentation of a new magnetic field therapy system for the treatment of human solid tumors with magnetic fluid hyperthermia.* Journal of Magnetism and Magnetic Materials, 2001. **225**(1-2): p. 118-126.

53. Varanda, L.C., et al., *Structural and magnetic transformation of monodispersed iron oxide particles in a reducing atmosphere.* Journal of Applied Physics, 2002. **92**: p. 2079.

54. Pratsinis, S.E. and S. Vemury, *Particle formation in gases: a review.* Powder Technology, 1996. **88**(3): p. 267-273.

55. Otsuka, H., Y. Nagasaki, and K. Kataoka, *PEGylated nanoparticles for biological and pharmaceutical applications.* Advanced Drug Delivery Reviews, 2003. **55**(3): p. 403-419.

56. Chilkoti, A., M.R. Dreher, and D.E. Meyer, *Design of thermally responsive, recombinant polypeptide carriers for targeted drug delivery.* Advanced Drug Delivery Reviews, 2002. **54**(8): p. 1093-1111.

57. Chouly, C., et al., *Development of superparamagnetic nanoparticles for MRI: effect of particle size, charge and surface nature on biodistribution.* Journal of Microencapsulation, 1996. **13**(3): p. 245-255.

58. Chatterjee, J., Y. Haik, and C.J. Chen, *Size dependent magnetic properties of iron oxide nanoparticles.* Journal of Magnetism and Magnetic Materials, 2003. **257**(1): p. 113-118.

59. Storm, G., et al., *Surface modification of nanoparticles to oppose uptake by the mononuclear phagocyte system.* Advanced Drug Delivery Reviews, 1995. **17**(1): p. 31-48.

60. Zhang, Y., N. Kohler, and M. Zhang, *Surface modification of superparamagnetic magnetite nanoparticles and their intracellular uptake.* Biomaterials, 2002. **23**(7): p. 1553-1561.

61. Zimmermann, U., J. Vienken, and G. Pilwat, *Development of drug carrier systems: electric field induced effects in cell membranes.* J. Electroanal. Chem, 1980. **116**: p. 553-574.

62. Freeman, J.A. and J.C. Geer, *Intestinal fat and iron transport, goblet cell mucus secretion, and cellular changes in protein deficiency observed with the electron microscope.* Digestive Diseases and Sciences, 1965. **10**(12): p. 1004-1023.

63. Gómez-Lopera, S.A., R.C. Plaza, and A.V. Delgado, *Synthesis and Characterization of Spherical Magnetite/Biodegradable Polymer Composite Particles.* Journal of Colloid and Interface Science, 2001. **240**(1): p. 40-47.

64. Wong, W.S., *Practical MRI, Magnetic Resonance Imaging: A Case Study Approach*

1987: Aspen Publishers.

65. Mitchell, D.G. and M.S. Cohen, *MRI principles*. 1998: W.B. Saunders Company.

66. Vlaardingerbroek, M.T., *Magnetic Resonance Imaging: Theory and Practice*. 1999: Springer.

67. Friebolin, H., *Basic one-and two-dimensional NMR spectroscopy.* 1998.

68. Weinmann, H.J., et al., *Characteristics of gadolinium-DTPA complex: a potential NMR contrast agent.* AJR Am J Roentgenol, 1984. **142**(3): p. 619-24.

69. Josephson, L., et al., *High-efficiency intracellular magnetic labeling with novel superparamagnetic-Tat peptide conjugates.* Bioconjug Chem, 1999. **10**(2): p. 186-91.

70. Reimer, P. and P. Landwehr, *Non-invasive vascular imaging of peripheral vessels.* European Radiology, 1998. **8**(6): p. 858-872.

71. Zhao, M., et al., *Non-invasive detection of apoptosis using magnetic resonance imaging and a targeted contrast agent.* Nature Medicine, 2001. **7**: p. 1241-1244.

72. Thompson, C.B., *Apoptosis in the pathogenesis and treatment of disease.* Science, 1995. **267**(5203): p. 1456-1462.

73. Weissleder, R., et al., *Superparamagnetic iron oxide: pharmacokinetics and toxicity.* AJR Am J Roentgenol, 1989. **152**(1): p. 167-73.

74. Reimer, P., et al., *Clinical results with Resovist: a phase 2 clinical trial.* Radiology, 1995. **195**(2): p. 489-96.

75. Lesniak, C., et al., *Nanoscale particles having an iron oxide-containing core enveloped by at least two shells*. 2005, US Patent 6,979,466.

76. Silva, L.P., et al., *Kinetic of magnetic nanoparticles uptake evaluated by morphometry of mice peritoneal cells.* Journal of Magnetism and Magnetic Materials, 2005. **289**: p. 463-465.

77. Passirani, C., et al., *Interactions of nanoparticles bearing heparin or dextran covalently bound to poly (methyl methacrylate) with the complement system.* Life Sciences, 1998. **62**(8): p. 775-785.

78. Matuszewski, L., et al., *Cell Tagging with Clinically Approved Iron Oxides: Feasibility and Effect of Lipofection, Particle Size, and Surface Coating on Labeling Efficiency.* Radiology, 2005: p. 2351040094.

79. Lianjun Shi, C.B., *Acid-Labile polyvinylamine Micro-and Nanogel Capsules.* Macromolecules, 2007. **40**: p. 4635-4643.

80. Kang, Y.S., S. Risbud, and J.F. Rabott, *Synthesis and characterization of nanometer-size Fe3O4 and Fe2O3 particles.* Chem Mater, 1996. **8**: p. 2.

81. Frisken, B.J., *Revisiting the method of cumulants for the analysis of dynamic light-scattering data.* Appl. Opt, 2001. **40**: p. 4087-4091.

82. Wang, K.L., J.H. Burban, and E.L. Cussler, *Hydrogeis as Separation Agents.*

83. Xu, Z.Z., et al., *Encapsulation of nanosized magnetic iron oxide by polyacrylamide via inverse miniemulsion polymerization.* Journal of Magnetism and Magnetic Materials, 2004. **277**(1-2): p. 136-143.

84. Santra, S., et al., *Synthesis and Characterization of Silica-Coated Iron Oxide Nanoparticles in Microemulsion: The Effect of Nonionic Surfactants.* Magn. Reson. Med, 1992. **24**: p. 75.

85. Zaitsev, V.S., et al., *Physical and chemical properties of magnetite and magnetite-macromolecule nanoparticles and their colloidal dispersions.* J. Coll. Interf. Sci, 1999. **212**: p. 49–57.

86. Arias, J.L., et al., *Synthesis and characterization of poly (ethyl-2-cyanoacrylate) nanoparticles with a magnetic core.* Journal of Controlled Release, 2001. **77**(3): p. 309-321.

87. Pardoe, H., et al., *Structural and magnetic properties of nanoscale iron oxide particles synthesized in the presence of dextran or polyvinyl alcohol.* Journal of Magnetism and Magnetic Materials, 2001. **225**(1-2): p. 41-46.

88. Kamruzzaman Selim, K.M., et al., *Surface modification of magnetite nanoparticles using lactobionic acid and their interaction with hepatocytes.* Biomaterials, 2007. **28**(4): p. 710-716.

89. Popplewell, J. and L. Sakhnini, *The dependence of the physical and magnetic properties of magnetic fluids on particle size.* Journal of Magnetism and Magnetic Materials, 1995. **149**(1): p. 72-78.

90. Brunot, C., et al., *Cytotoxicity of polyethyleneimine (PEI), precursor base layer of polyelectrolyte multilayer films.* Biomaterials, 2007. **28**(4): p. 632-640.

4. Appendix

Appendix I

2.2. Synthesis of Non-Degradable Cross-Linker

To synthesize 2-(N-vinylformamido)ethyl ether NVEE (cross-linker) a mixture of N-vinylformamide (21 g), potassium t-butoxide (35.44 g) and dicyclohexyl-18-crown-6 (3 g) in anhydrous THF was stirred vigorously at room temperature for 45 minutes to activate secondary amine group and then cooled in an ice bath. Bis(2-bromthyl)ether (27.8 g) was added drop wise, and the mixture was stirred at room temperature for 72 hours. In the next step, potassium bromide salt was removed by filtration and then the reaction mixture was concentrated under vacuum and diluted with 300 mL of water. The crude product was obtained by extraction with chloroform five times (50 mL× 3). The combined organic layers were washed twice with brine and dried over anhydrous sodium sulfate. The resulting product was recovered after concentration in a vacuum distillation column and purification by chromatography on silica (ethyl acetate/hexane: 8:2 v/v).

Appendix II

Monomer (µL)	Crosslinker (µL)	Surfactant (gr)	water (µL)	PNVF hydrodynamic size (nm)
350	50	7.1	165	112
350	50	14.2	165	259
350	50	21.3	165	141
350	50	28.4	165	279
350	50	21.3	42.5	182
350	50	21.3	20	251
166.5	33.5	21.3	165	209
150	50	21.3	165	216